ORIGINAL ARTICLE



Investigating the developmental onset of regenerative potential in the annelid *Capitella teleta*

Alicia A. Boyd | Elaine C. Seaver 🗅

Whitney Laboratory for Marine Bioscience, University of Florida, St. Augustine, Florida, USA

Correspondence

Elaine C. Seaver, Whitney Laboratory for Marine Bioscience, University of Florida, 9505 N Ocean Shore Blvd, St. Augustine, FL 32080. USA.

Email: seaver@whitnev.ufl.edu

Abstract

An animal's ability to regrow lost tissues or structures can vary greatly during its life cycle. The annelid Capitella teleta exhibits posterior, but not anterior, regeneration as juveniles and adults. In contrast, embryos display only limited replacement of specific tissues. To investigate when during development individuals of C. teleta become capable of regeneration, we assessed the extent to which larvae can regenerate. We hypothesized that larvae exhibit intermediate regeneration potential and demonstrate some features of juvenile regeneration, but do not successfully replace all lost structures. Both anterior and posterior regeneration potential of larvae were evaluated following amputation. We used several methods to analyze wound sites: EdU incorporation to assess cell proliferation; in situ hybridization to assess stem cell and differentiation marker expression; immunohistochemistry and phalloidin staining to determine presence of neurites and muscle fibers, respectively; and observation to assess re-epithelialization and determine regrowth of structures. Wound healing occurred within 6 h of amputation for both anterior and posterior amputations. Cell proliferation at both wound sites was observed for up to 7 days following amputation. In addition, the stem cell marker vasa was expressed at anterior and posterior wound sites. However, growth of new tissue was observed only in posterior amputations. Neurites from the ventral nerve cord were also observed at posterior wound sites. De novo ash expression in the ectoderm of anterior wound sites indicated neuronal cell specification, although the absence of elav expression indicated an inability to progress to neuronal differentiation. In rare instances, cilia and eyes re-formed. Both amputations induced expanded expression of the myogenesis gene MyoD in preexisting tissues. Our results indicate that amputated larvae complete early, but not late, stages of regeneration, which indicates a gradual acquisition of regenerative ability in C. teleta. Furthermore, amputated larvae can metamorphose into burrowing juveniles, including those missing brain and anterior sensory structures. To our knowledge, this is the first study to assess regenerative potential of annelid larvae.

KEYWORDS

cell division, larva, metamorphosis, regeneration, vasa

Resumo

La capacidad de un animal para regenerar tejidos o estructuras que se pierden puede variar mucho durante su ciclo de vida. El anélido *Capitella teleta* exhibe regeneración

posterior, pero no anterior, tanto en juvenil como en adulto. En contraste, los embriones sólo muestran un reemplazo limitado de tejidos específicos. Para investigar cuándo los individuos de C. teleta son capaces de regenerarse durante su desarrollo, evaluamos hasta qué punto las larvas pueden hacerlo. Nuestra hipótesis fue que las larvas exhiben un potencial de regeneración intermedio y muestran algunas características de la regeneración juvenil, pero no reemplazan con éxito todas sus estructuras perdidas. Después de la amputación se evaluó el potencial de regeneración anterior y posterior de las larvas. Utilizamos varios métodos para analizar el área de la amputación: incorporación de EdU para evaluar la proliferación celular; hibridación in situ para evaluar la expresión de células madre y marcadores de diferenciación; inmunohistoquímica y tinción con faloidina para determinar la presencia de neuritas y fibras musculares, respectivamente; y observación para evaluar la reepitelizacion y determinar si hay un nuevo crecimiento de las estructuras amputadas. La cicatrización de la herida se produjo dentro de las 6 horas posteriores a la amputación, tanto para la amputación anterior como para la posterior. Se observó proliferación celular en ambos sitios de la amputación hasta 7 días después del corte. Además, el marcador de células madre vasa se expresó en los sitios de la amputación anterior y posterior. Sin embargo, el crecimiento de tejido nuevo se observó sólo en amputaciones posteriores. También se observaron neuritas del cordón nervioso ventral en los sitios de la amputación posterior. La expresión de novo de ash en el ectodermo de los sitios de la amputación anterior indicó especificación de células neuronales, aunque la ausencia de expresión de elav indicó una incapacidad para progresar hacia la diferenciación neuronal. En casos raros, los cilios y los ojos se formaron de nuevo. Ambas amputaciones indujeron una amplia expresión del gen de miogénesis MyoD en tejidos preexistentes. Nuestros resultados indican que las larvas amputadas completan etapas tempranas, pero no tardías, de regeneración, lo que indica una adquisición gradual de la capacidad regenerativa en C. teleta. Además, las larvas amputadas pueden metamorfosearse en juveniles excavadores, incluso aquellos a los que les falto el cerebro y las estructuras sensoriales anteriores. Hasta donde sabemos, este es el primer estudio que evalúa el potencial regenerativo en larvas de anélidos.

1 | INTRODUCTION

Regeneration is the replacement of tissues or structures after injury or amputation. The ability to regenerate lost tissues varies throughout the animal kingdom (Alvarado, 2000). For example, animals such as planarians and hydra can completely reform any lost structure with hardly any restriction (i.e., whole-body regeneration) (Reddien, 2018; Reddy et al., 2019). Other animals have a more restrictive capacity to regenerate and re-form only specific structures, such as limbs in crustaceans (Alwes et al., 2016) and amphibians (Brockes, 1997; Byrnes, 1904; Singer, 1954). Finally, some animals, such as the leech, display almost no regenerative capabilities following bisection (Özpolat & Bely, 2016). Here, we briefly review differences in regeneration potential across animal life cycles and describe the need to examine regeneration more carefully in pre-adult stages. We

highlight annelids as a clade with exceptional regeneration diversity and introduce *Capitella teleta* as a prime candidate in which to examine how regeneration changes during the life cycle of an indirect developer.

Most published surveys of regeneration ability focus on adult stages, whereas few studies examine regeneration potential at earlier stages of the life cycle. Several questions emerge when one considers regeneration potential across the life cycle. In animals with a biphasic life cycle, does regeneration ability differ among embryos, larvae, and adults? If so, when in the life cycle is the regeneration program activated: during larval stages or after metamorphosis? Are there conserved trends of increasing or decreasing regeneration abilities across the life cycle? From a developmental perspective, one might expect a trend of decreasing regeneration abilities through the life cycle as embryonic cells become committed to distinct cell types, undergo

terminal differentiation, and lose their pluripotency. As a result, there would be progressive loss in the ability to replace tissues (e.g., appendages, nervous system, and heart) (Porrello et al., 2011; Walters & Zuo, 2013; Yun, 2015). However, in animals with indirect life cycles, larvae and adults often have distinct tissues, and adult tissue formation requires the retention of progenitors or multipotent stem cells through the larval phase (Peterson et al., 1997). The presence of stem cells in larvae suggests the possibility that animals with indirect development may have greater regeneration potential relative to direct developing species.

Of the published studies that examine regeneration in larvae, the vast majority focus on deuterostomes and suggest that the pattern of regeneration ability in larvae and adults is complex. For example, frogs in the genus Xenopus can replace specific tissues (i.e., appendages, heart, brain, lens) as larvae, but as they mature this regeneration ability is lost, which is a pattern similar to that observed in direct developers (Harrison, 1898; Phipps et al., 2020). However, in the crinoid Antedon bifida (= Antedon rosacea) the larvae exhibit limited ability to regenerate following bisection, but adults are capable of whole-body regeneration (Carnevali, 2006; Carnevali et al., 1993). Furthermore, sea stars exhibit whole-body regeneration during larval, juvenile, and adult stages (Carnevali, 2006). Other animals have a more dynamic change in regenerative ability through their life cycle. In Ciona intestinalis, larvae lack regenerative abilities, yet adults exhibit structural regeneration only to progressively lose this ability with advanced age (Jeffery, 2015). A broad understanding of how regeneration ability relates to the life cycle is largely unexplored, and it is critical to sample pre-adult stages in animal taxa in which adults have the ability to regenerate, particularly from protostome lineages.

Annelids are segmented worms that have a wide range of regenerative abilities as adults. Some lack the ability to regenerate following transverse amputation, others regenerate either anterior or posterior segments only, or even undergo whole-body regeneration (Bely, 2006). A systematic review of annelid regenerative ability revealed that anterior and posterior regeneration are widespread across the phylum, alongside numerous examples of evolutionary loss of regeneration (Bely, 2006). Furthermore, it is likely that both anterior and posterior regeneration are ancestral for adult annelids (Zattara & Bely, 2016). Although some studies have characterized regeneration during juvenile stages (del Olmo et al., 2022; Kostyunchenko, 2022; Planques et al., 2019), to our knowledge, a broad assessment of larval regenerative potential is lacking for annelids.

Capitella teleta BLAKE ET AL., 2009 is an annelid capable of posterior regeneration and has an indirect life cycle (Seaver, 2022). Previous studies hint at changes in the ability of individuals of *C. teleta* to replace lost structures across their life cycle. Juvenile and adult worms regenerate following bisection along the main body axis (de Jong & Seaver, 2016; Giani et al., 2011). In contrast, early-stage embryos do not regulate following deletion of individual precursor cells (Pernet et al., 2012), apart from eye and germline precursor cells (Dannenberg & Seaver, 2018; Yamaguchi et al., 2016). It is unknown when individuals of *C. teleta* gain regenerative ability, or to what degree larvae might be capable of regeneration.

Following embryogenesis in *C. teleta*, a non-feeding lecithotrophic larva forms. Lecithotrophic larvae often have "abbreviated developmental times" (Vickery et al., 2001), which characterizes the larval phase in *C. teleta* of \sim 5–6 days in duration. Larvae are characterized by trochal ciliated bands that divide the body into three regions along the anterior–posterior axis: the head, the segmented trunk, and the pygidium. The prototroch separates the head from the trunk and the telotroch separates the trunk from the pygidium (Figure 1A,B) (Seaver et al., 2005). These two ciliary bands are composed of long cilia. A third ciliary band, the neurotroch, runs along the ventral midline of the trunk and is composed of short cilia. Short cilia are also present in the pygidium. Larvae use the prototroch and telotroch to swim in the water column, which aids in dispersal.

During larval stages, the adult centralized nervous system, musculature, digestive system, and initial systems mature (Meyer et al., 2010). A previously described staging system uses morphological features to identify nine distinct stages of embryonic (Stages 1-3) and larval development (Stages 4-9) (Seaver et al., 2005). In C. teleta, the development of the centralized nervous system is initiated in late embryogenesis. A ladder-like ventral nerve cord (VNC) positioned along the midline of the trunk forms and is connected to the brain by a pair of circumoral nerves (Meyer et al., 2015; Seaver et al., 2005). The body wall musculature is organized segmentally with circular and longitudinal muscles, and the first muscle fibers appear at the beginning of larval life (Stage 4). Two pigmented eyes appear at Stage 5 and are located lateral and anterior to the prototroch (Meyer et al., 2010; Yamaguchi et al., 2016). Gut organogenesis becomes visibly pronounced between Stages 6-9. The foregut consists of the mouth, buccal cavity, pharynx (morphogenesis in Stage 7), and esophagus (Boyle & Seaver, 2008; see Figure 1A and Figure 1B). In Stages 8-9, the midgut differentiates. becoming olive green and stereotypically coiled (Figure 1B). Stage 6 larvae have ~10 segments, generating one segment a day until there are 13 segments present in Stage 9 larvae (Seaver et al., 2005). Larval development concludes when Stage 9 larvae metamorphose into burrowing juvenile worms (Cohen & Pechenik, 1999; Seaver et al., 2005).

We sought to determine when regeneration potential is initiated during the life history of C. teleta. We hypothesized that larvae may have limited regeneration potential distinct from that of juveniles and adults. We anticipated that larvae would display early stages of regeneration without successfully replacing lost tissues and structures. This would suggest that individuals of C. teleta acquire regenerative ability gradually through the life cycle. To test our hypothesis, we developed an amputation protocol for larvae to investigate both anterior and posterior regeneration. We characterized larval responses to amputation by making direct comparisons with regeneration events in juveniles. At the wound site, we documented epithelial wound healing, evaluated cell proliferation by EdU incorporation, analyzed changes in neuronal organization with antibody labeling, and visualized musculature with phalloidin staining. We also conducted in situ hybridization experiments to analyze expression of the neuronal specification and differentiation gene markers ash1 and elav, respectively, as well as examined muscle fate and differentiation through analysis of the MyoD gene.

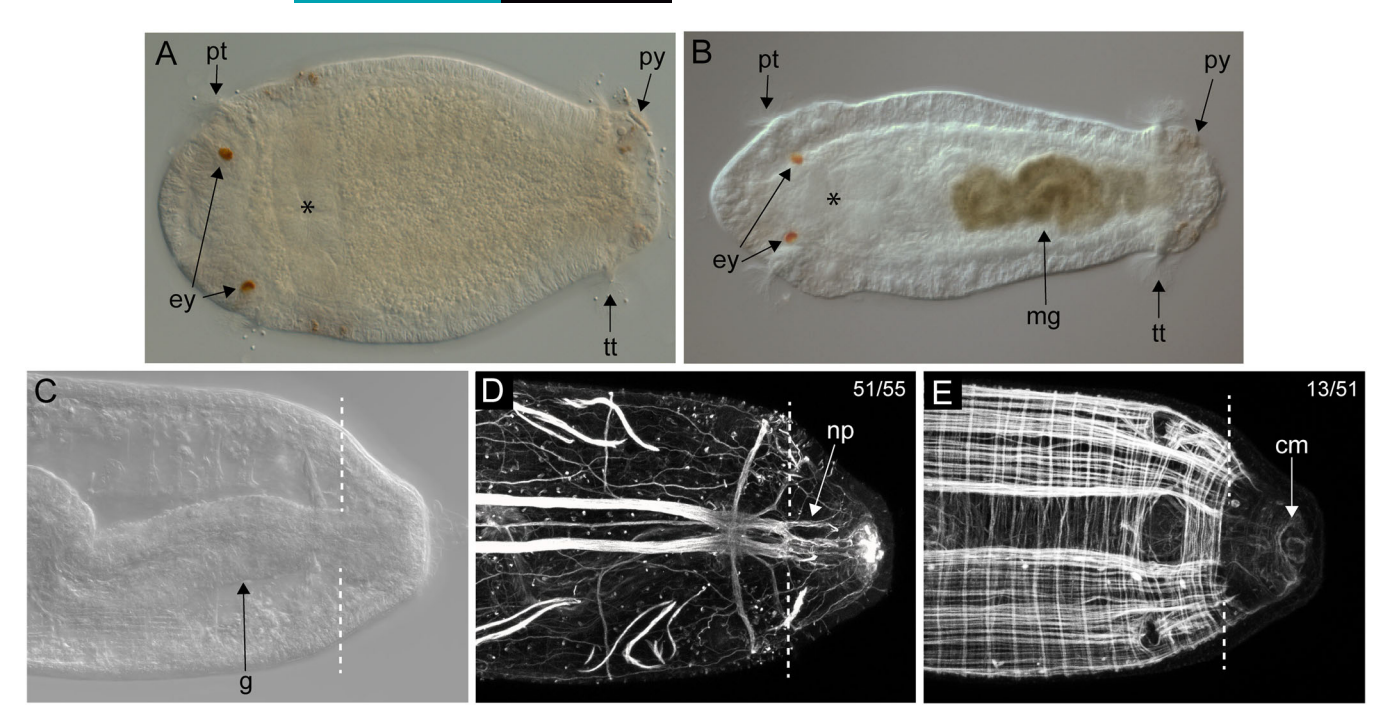


FIGURE 1 Larvae and regenerating juveniles of *Capitella teleta*. All images are oriented in ventral view with anterior to the left. (A) Stage 6 larva. (B) Stage 9 larva. (C-E) Images of the posterior end of a regenerating juvenile 3 days post-amputation, from the same specimen. (C) Differential interference contrast image showing regeneration of new tissue. (D) Nervous system visualized with anti-acetylated tubulin antibody labeling. (E) Phalloidin staining shows muscle fibers with few fibers in the regenerating tissue. The white dotted lines indicate amputation sites. The number of animals scored that resembled the image shown (out of the total number of animals examined) is noted in the top right corner. The asterisk marks the position of the mouth. cm, circular muscle; ey, eyes; g, gut; mg, midgut; np, neural projection; pt, prototroch; py, pygidium; tt, telotroch.

2 | METHODS

2.1 | Animal care

As described in previous work (Grassle & Grassle, 1976), a colony of *Capitella teleta* was maintained in the laboratory at 19°C in glass finger bowls containing filtered seawater (FSW) and a thin layer of marine mud. Using forceps, larvae were dissected from the brood tubes of healthy females. Larvae from a single brood tube developed synchronously, and the number of individuals per brood averaged 100–250 individuals. Brood tubes were maintained in FSW until the desired age for amputation or treatment.

2.2 | Amputations

Stage 6 larvae were used for amputation experiments. Larvae were developmentally staged following a standard staging system (Seaver et al., 2005). Stage 6 is characterized by presence of yolk in the anterior portion of the larva, swimming behavior with a positive phototactic response, and lack of chaetae. Prior to amputation, larvae were incubated in 1:1 MgCl₂: FSW for 10 min to inhibit muscle contraction. Individual larvae were transferred to a 60-mm petri dish lid filled with a methyl cellulose solution (0.3 g methyl cellulose in 15 mL filtered seawater) for amputation. Additional methyl cellulose was added as

necessary to achieve immobilization. Glass capillary tubes (50 µL, Becton Dickinson and Company) were heated over a flame and pulled into thin, flexible, sharp tips to use as amputation tools. Larvae were amputated with a single continuous, downward motion. Cut sites for anterior amputations and eye amputations were located just posterior to the prototroch, removing the anterior third of the animal (i.e., brain, eyes, and prototroch). Cut sites for posterior amputations were located $\sim 2/3$ of the body length posterior to where the width of the trunk decreases and slopes to the pygidium, effectively removing the posterior growth zone, telotroch, and pygidium. Following amputation, each individual was visually inspected for correct cut location and complete separation of the two tissue fragments. Amputated larvae were transferred to a 60-mm petri dish containing 1:1 0.37 M MgCl₂: FSW and incubated for a minimum of 1 h. Larvae were then washed into FSW containing 60 μg/mL penicillin and 50 μg/mL streptomycin (Sigma-Aldrich Co.) (P/S) and raised at 19°C. Filtered seawater with antibiotics was replaced daily, and vitality and swimming behavior were monitored daily. For each amputation experiment, age-matched larvae from the same brood tube as experimental animals were raised as uncut controls. In a typical experiment, 40-60 individuals from a single brood were amputated. For posterior amputations, amputations were performed on sets of individuals from at least 10 broods, and for anterior amputations, sets of individuals from at least five broods were amputated. Both anterior- and posterior-amputated larvae had high rates of survivorship, ranging from 75% (37/50) to 85% (28/33).

Two-week-old juveniles were prepared for amputation by incubation in 1:1 MgCl₂: FSW for 10 min. Individual worms were transferred to a platform of black dissecting wax (American Educational Products, Fort Collins, CO, USA) in the lid of a 35 mm plastic dish for amputation in a drop of 1:1 MgCl₂: FSW. For eye amputations, worms were amputated immediately anterior to the mouth, removing the eyes and brain. Amputations for posterior regeneration were at the boundary between Segments 10 and 11. Individual worms were visually inspected for the correct cut site and successful separation before being transferred to a 60-mm petri dish and incubated in 1:1 MgCl₂: FSW for a minimum of 1 h. The juveniles were then washed into FSW and moved to a 60-mm petri dish containing mud and FSW and raised at 19°C for 1 week. For analysis, juvenile worms were sifted from the mud and placed into a petri dish of 1:1 MgCl₂: FSW. Worms were fixed with 4% paraformaldehyde (PFA) in FSW for 30 min before being washed into phosphatebuffered saline (PBS). Fixed juveniles were scored for pigmented eye cells before being processed for antibody labeling.

2.3 | Cell proliferation assay

Larvae were incubated in EdU (Click-iT EdU Alexa Fluor 488 imaging kit - Invitrogen) diluted in FSW to a final concentration of 3 μ M at room temperature for 30 min. Larvae were then washed into a 1:1 MgCl₂: FSW solution for 10 min and then fixed in 4% PFA for 30 min. Afterward, they were rinsed into PBS and incubated for 20 min at room temperature in PBS + 0.05% Triton-X-100 with rocking. The specimens were incubated in the commercially provided EdU reaction buffer for 30 min, rocking at room temperature. Finally, larvae were washed into PBS and stored at 4°C until further analysis.

2.4 | EdU quantification

Quantification of EdU- and Hoechst-stained cells in uncut and amputated larvae was conducted by importing Z-stacks generated from confocal microscopy (see section 2.9, Microscopy and imaging analysis) into ImageJ software. Using Hoechst and DIC channels to establish boundaries, each image was cropped around the perimeter of the animal. The channels were split and treated separately to optimize cell counting. The threshold for each channel was adjusted manually to minimize background and enhance distinction of individual cells. Afterward, a mask and watershed application were applied to each channel. The resulting image was divided into three equal sections along the anterior-posterior axis using the Montage to Stack application. The modified images were compiled into 20 slice projections (20 µm total) before being counted automatically by Analyze Particles in the Analyze menu. Each 20-µm Z-stack was counted, with the results automatically summarized via section. Manual inspection eliminated any cells that were counted twice by the software. Results were manually compiled by channel and section for each animal, as well as for each time point. A ratio of EdU-stained cells to Hoechst-stained cells was calculated for each time point from the ImageJ cell count

summaries. Averages of each body section (anterior, middle, and posterior) for each time point (uncut controls, 6 h post-amputation, 3 days post-amputation, and 5 days post-amputation) were calculated separately. Ten randomly selected larvae were scored for each time point, and a mean value was calculated for each body section across individuals. Each body section of uncut controls was compared with corresponding body sections of amputated animals. One-way weighted ANOVA statistical tests were performed using VassarStats (Lowry, 2023) to test for significance between the control and amputation group of interest.

2.5 | Antibody labeling and phalloidin staining

Amputated larvae or juveniles were incubated in a 1:1 MgCl₂: FSW solution for 10 min and fixed in 4% paraformaldehyde in FSW for 30 min. Animals were washed several times into PBS to remove fixative and then washed into a PBS + Triton solution (PBT) (0.1% Triton-X-100 for larvae and 0.2% Triton-X-100 for juveniles). Animals were transferred to a three-well glass depression plate and incubated in a solution of 10% heat-inactivated normal goat serum in PBT at room temperature, with rocking for 45-60 min. For antibody labeling, the anti-acetylated tubulin antibody (goat anti-mouse, Sigma-Aldrich Co.) was diluted 1:400 in block solution (10% heated-treated goat serum in PBT), and incubated with larvae or juveniles at room temperature for 2 h or overnight at 4°C. Following multiple washes in PBT (four times in PBT for 30 min each), a secondary antibody (goat anti-mouse red 594, Invitrogen) was diluted 1:400 in block solution and added to animals prior to incubation for 2-4 h, with rocking at room temperature or overnight at 4°C. The 22C10 antibody (Goat anti-mouse, Developmental Studies Hybridoma bank; 22C10 was deposited to the DSHB by Benzer, S. /Colley, N. [DSHB Hybridoma Product 22C10]) was diluted 1:200 in block solution, added to animals and incubated overnight at 4°C. Following multiple washes in PBT over 2 h, the secondary antibody (goat anti-mouse green 488 - Invitrogen) was diluted 1:400 in block solution, added to animals and incubated overnight at 4°C. Following incubation in secondary antibody, larvae were rinsed two to three times in PBT and then washed four times in PBT for 30 min each wash. For phalloidin staining, specimens were incubated in a 1:400 dilution of phalloidin (Alexa Fluor 488 phalloidin, Invitrogen) in PBT. Specimens were incubated on a rocker at room temperature for 45-60 min before being washed twice in PBT for 30 min each wash. Animals were cleared in 80% glycerol in PBS with 1 µg/mL Hoechst-33342 (Molecular Probes) overnight prior to imaging.

2.6 Whole mount in situ hybridization

Larvae collected at different time points following amputation were incubated in a 1:1 MgCl₂: FSW solution for 10 min and then fixed in 4% paraformaldehyde overnight at 4° C. Fixative was removed by multiple rinses in PBS, and then larvae were gradually washed into 100% methanol and stored at -20° C. Whole mount in situ hybridization

was performed following a previously published protocol (de Jong & Seaver, 2017). DIG-labeled RNA probes were generated with the MegaScript SP6 or T7 Transcription kit (Invitrogen) according to manufacturer instructions. The following probes and their working concentrations were used: ash1 at 3 ng/µL, MyoD at 0.5 ng/µL, vasa at 1 ng/ μ L, and elav at 2 ng/ μ L. Animals were hybridized for \sim 24-48 h with riboprobe at 65°C. Each RNA probe was visualized by exposure to an anti-digoxigenin-alkaline phosphatase conjugate antibody (Roche) prior to exposure to a color reaction solution containing NBT/BCIP (nitro blue tetrazolium chloride/5-bromo-4-chloro-3-indolyphosphate) and visually monitored for optimal development time. For each sample, uncut control larvae were developed for the same duration as experimental, amputated larvae. Color reactions were terminated following washes of PBT followed by a final fixation in 4% PFA in FSW for 30 min. Tissue was cleared in 80% glycerol in PBS plus 0.1 µg/mL Hoescht to stain nuclei, and then individuals were placed on microscope slides for analysis and imaging. At least two independent repetitions were performed for each gene.

2.7 | Tissue and cilia measurements

To measure tissue formation in amputated larvae, confocal images were analyzed using ImageJ software. Multiple measurements were made on each specimen. The nervous system was measured from the cut site to the position most distal from the cut site that contained neurites. Muscle measurements were taken from the cut site to the position most distal from the cut site that contained phalloidin-positive fibers. Changes in body width were calculated by making two measurements per specimen: the first measurement was taken at the axial level of the mouth, and the second was just posterior to the cut site. Gut measurements were made from the posterior end of the pigmented midgut to the posterior edge of the posterior ectoderm. For anterior amputations, the muscle and nervous system were measured on larvae 6 h post-amputation (n = 8) and 3 days post-amputation (n = 10). For posterior amputations, the muscle, nervous system, and changes in body width were measured on larvae 6 h post-amputation (n = 7) and 5 days post-amputation (n = 10) larvae. Additionally, the posterior edge of the midgut was used as a landmark for measurements in larvae 5 days post-amputation and Stage 9 larvae at 6 h post-amputation (n = 10). Unpaired t-test, with two-tailed hypothesis statistical tests were performed using the Social Science Statistics software (Social Science Statistics, 2023) to test for significance between the uncut control and experimental amputation group of interest.

The cilia of larvae were measured using ImageJ software on confocal image projections. Individual labeled cilia of the prototroch, neurotroch, telotroch, and pygidium were traced. Lines resulting from the trace were then measured using the measure tool found under Analyze. At least three cilia for each ciliary band type were measured in a representative individual, and three individuals were measured, resulting in a total of at least nine measurements for each of the prototroch, telotroch, neurotroch, and pygidium ciliary lengths. The range of cilia lengths across the nine measurements is reported (see Section 3).

2.8 | Metamorphosis assays

Metamorphosis is rapidly induced in Stage 9 larvae of C. teleta by exposure to vitamin B supplements (Burns et al., 2014). A single multivitamin (Centrum Men Multivitamin) was dissolved in 200 mL FSW and stored at room temperature. Stage 9 larvae were amputated one day prior to exposure to vitamin B. To test whether amputated larvae are capable of successful metamorphosis, uncut, anteriorly amputated, and posteriorly amputated larvae were exposed to the multivitamin solution containing vitamin B. Larvae were placed in a 30-mm petri dish in FSW. Most of the FSW was removed from the dish and replaced with 3 mL of the multivitamin solution. Animals were incubated in the vitamin solution for 20-30 min. The multivitamin solution was removed by a minimum of three washes with FSW (2 mL/wash), and then animals were individually scored for settlement and metamorphosis. Successful settlement and metamorphosis were defined as cessation of swimming behavior and initiation of burrowing, loss of the prototroch and telotroch ciliary bands, and elongation of the body.

2.9 | Microscopy and imaging analysis

Larvae were imaged with a Zeiss 710 confocal microscope, with $4\times$ bidirectional and unidirectional scan settings for the green and red lasers. Z-stacks were compiled using ImageJ software (Schindelin et al., 2012). Differential interference contrast microscopy images were captured on a Zeiss AxioSkop II motplus compound microscope (Zeiss) coupled with a SPOT FLEX digital camera (Diagnostic Instruments Inc). Multiple focal planes were merged for DIC images using Helicon Focus software (Helicon Focus 7). Images were cropped and processed for brightness and contrast with Photoshop (Adobe Photoshop 2020) or Illustrator (Adobe Illustrator 2020). Figures were composed in Adobe Illustrator (Adobe Illustrator 2020).

3 | RESULTS

3.1 | Characteristics of successful regeneration in *C. teleta*

To characterize larval regenerative potential, we looked to the juvenile posterior regeneration program in *C. teleta* to define features of successful regeneration. Juveniles of *C. teleta* maintain three conserved sequential stages of posterior regeneration: wound healing, cell proliferation, and differentiation of new tissues (de Jong & Seaver, 2016). Following amputation in juveniles, the wound heals in 4–6 h and thereafter forms a blastema (Figure 1C) (de Jong & Seaver, 2016). Neuronal projections extend from the VNC into the wound site as early as 2 days post-amputation (Figure 1D; see also de Jong & Seaver, 2016). In regenerating juveniles, the thickness of the connective nerve decreases dramatically at the point of amputation, with multiple thin neural projections extending from the old VNC tissue

into the wound tissue and thereafter into the blastema or new tissue. This change in VNC thickness indicates the position of the cut site. Localized cell proliferation is also observed at the wound site by 2 days post-amputation and persists for several days as new segments form (de Jong & Seaver, 2016). We observed that the density of circular and longitudinal muscle fibers decreased abruptly at the wound site at 3 days post-amputation (Figure 1E). Circular and longitudinal muscle fibers are absent between the posterior boundary of the old tissue and phalloidin-positive fibers at the posterior end of the animal. The decrease in muscle fibers spatially align with the decrease in thickness of the connective nerves of the VNC. After \sim 7 days, additional segments are formed that contain organized ganglia, peripheral nerves, circular and longitudinal muscles, digestive tissue, and other differentiated tissues (de Jong & Seaver, 2016).

3.2 | Amputation responses in larvae and subsequent development

To assess the regenerative potential of larvae of *C. teleta*, sites were selected for both anterior and posterior amputations in which we removed $\sim 1/3$ of the body (Figure 2A). Initial analysis focused on wound healing, which was identified by presence of a continuous epithelial layer covering the wound site and was the result of contraction of the severed edges of the body wall. To assess wound healing in amputated larvae, we analyzed Stage 6 larvae fixed at 2, 3, 5, and 6 h post-amputation for presence of a continuous epithelial layer covering

the wound site. Following anterior amputations, we observed consistent wound healing at 6 h post-amputation (54/54; Figure 2B). For posterior amputations, we observed wound healing as early as 2 h post-amputation (3/15); however, in most cases successful wound healing occurred \sim 6 h post-amputation (48/51; Figure 2C). In posterior amputations performed on Stage 9 larvae, successful wound healing also occurred by 6 h post-amputation (Figure 2D). Presence of tissue between the posterior edge of the pigmented midgut and the posterior epidermis of most animals indicated wound healing of the mesodermal layer by 6 h post-amputation.

Larvae survived multiple days following amputation and continued to develop toward metamorphic competency. Amputated larvae generally had high survivorship (~75%-85%) at 5 days post-amputation, and some anteriorly and posteriorly amputated animals survived up to 7 days post-amputation. Furthermore, amputated larvae continued to develop on schedule relative to uncut animals (Figure 2E,F). For example, in posteriorly amputated larvae, chaetae were present in the original tissue by 1 day post-amputation (comparable to Stage 7), pigmentation appeared in the midgut by 2 days post-amputation (comparable to Stage 8), and the midgut became coiled by 3 days post-amputation (comparable to Stage 9). Anteriorly amputated larvae also developed chaetae and a pigmented midgut, but the curvature of midgut, a hallmark of Stage 9 larvae (Boyle & Seaver, 2008; Seaver et al., 2005), was delayed by 1 day. The growth of anterior and posterior amputations differed. The shape of the body at the cut site in anterior amputations was frequently observed to be blunt, which was similar in shape to a specimen following wound healing (6 h post-

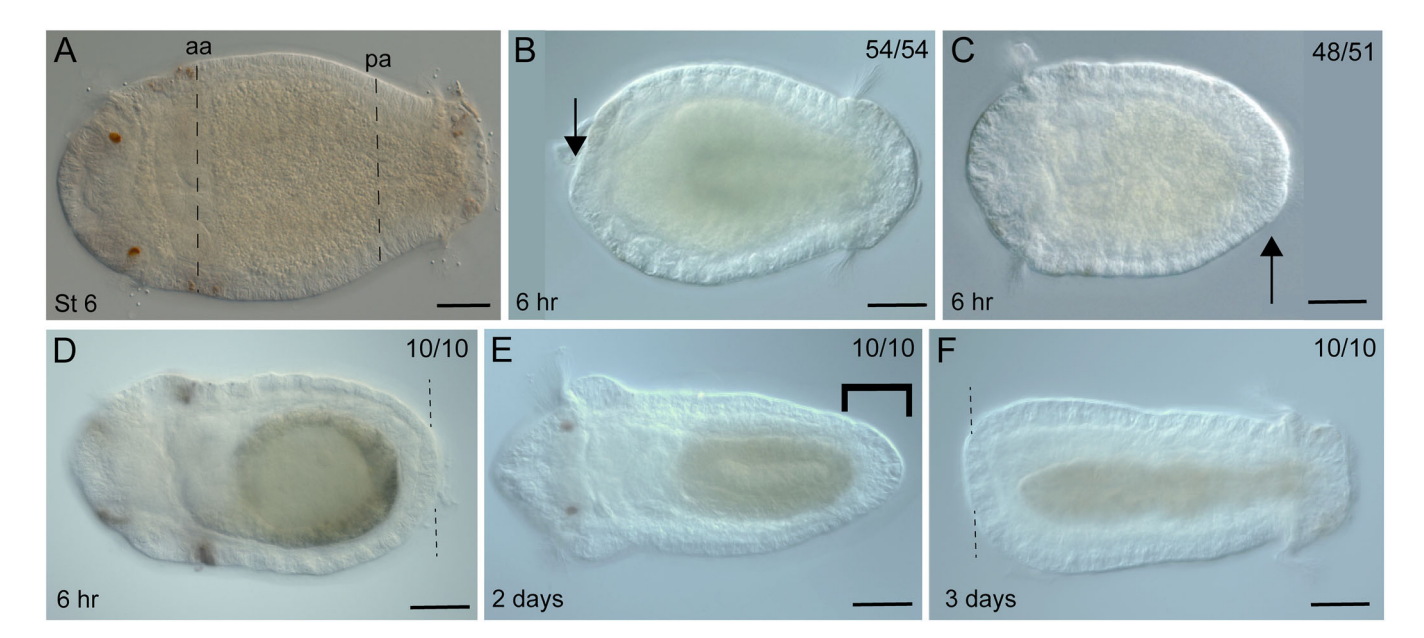


FIGURE 2 Amputated larvae of *Capitella teleta* undergo successful wound healing. All images are oriented in ventral view with anterior to the left. Arrows indicate the continuous layer of epithelium, indicative of successful wound healing. (A) Stage 6 uncut larva showing experiment design for amputations. (B) Stage 6 larva 6 h post-amputation, anterior amputation. (C) Stage 6 larva 6 h post-amputation, posterior amputation. (D) Stage 9 larva 6 h post-amputation, posterior amputation. (E) Stage 9 larva 2 days post-amputation, posterior amputation. (F) Larva 3 days post-amputation, anterior amputation. The black bracket represents the tissue between the gut and ectoderm. Amputation sites indicated by the black dashed lines. The number of animals scored that resembled the image shown (out of the total number of animals examined) is noted in the top right corner. Scale bars $= 50 \mu m$. aa, anterior amputation; pa, posterior amputation.

amputation) (Figure 2F), whereas the tissue distal to the cut site in posterior amputations had a rounded tapered shape (Figure 2E). The tapered shape in posterior amputations was different from the shape of the wound site in aged-matched individuals (Stage 9) fixed at 6 h post-amputation (compare Figure 2D,E). Our observations demonstrate that larvae not only survive removal of a third of their body, but they continue to develop with a similar time course to uncut animals.

3.3 | Cell proliferation

One key feature of regeneration is the birth of new cells in the region of the wound site. Larval development is a dynamic growth process that exhibits cell proliferation. Larvae in Stages 6 and 7 have a characteristic pattern of EdU incorporation following a 1 h exposure to EdU. Specifically, there are numerous EdU + cells distributed throughout the trunk, which straddle the midline (Figure 3A,B). In contrast, by

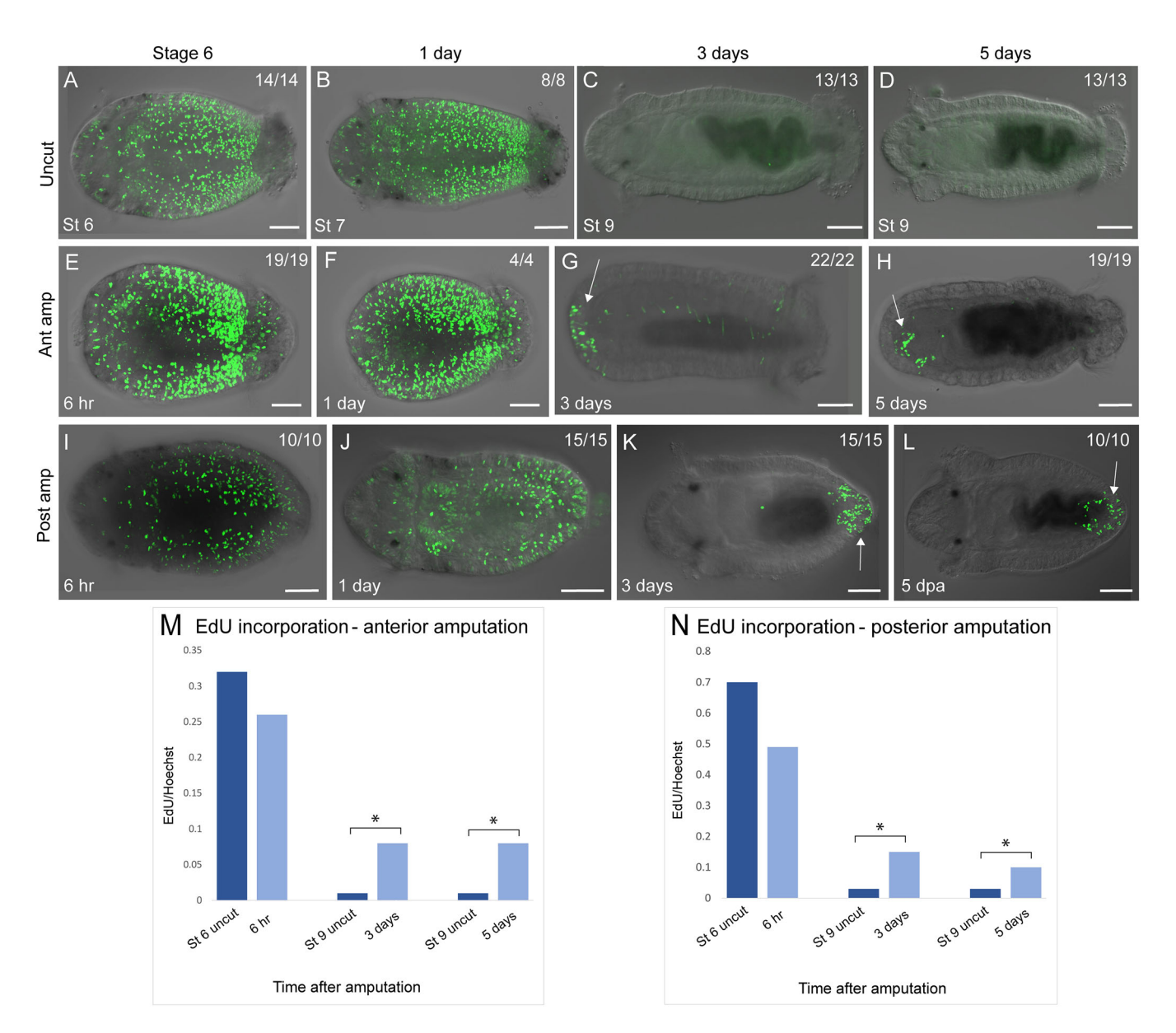


FIGURE 3 Localized cell proliferation near the amputation site in larvae of *Capitella teleta*. All images are oriented in ventral view with anterior to the left. Animals were exposed to EdU to label dividing cells. EdU+ cells are green. (A–D) Uncut controls: (A) Stage 6 larva; (B) Stage 7 larva; (C) Stage 9 larva; (D) Stage 9 larva. (E–H) Anterior amputations: (E) 6 h post-amputation; (F) 1 day post-amputation; (G) 3 days post-amputation; (H) 5 days post-amputation. (I–L) posterior amputations: (I) 6 h post-amputation; (J) 1 day post-amputation; (K) 3 days post-amputation; (L) 5 days post-amputation. (M, N) Quantification of EdU incorporation in anterior (M) and posterior (N) amputations, and comparison with uncut controls. Time after amputation is on the x axis and the ratio of EdU to Hoechst in cells is on the y axis. The white arrows indicate EdU + cells near the wound site. The developmental stage or time post-amputation is indicated in the bottom left corner of each panel. In (A)–(L), the number of animals scored that resembled the image shown (out of the total number of animals examined) is noted in the top right corner. Dark blue bars in the graphs represent uncut controls and light blue bars represent amputated animals; *p < 0.05. Scale bars = 50 μ m.

Stage 9, EdU + cells are not ordinarily observed, apart from a few cells in the midgut or hindgut and posterior growth zone (PGZ) (Figure 3C,D). To delineate between growth and a response to amputation, we compared age-matched, uncut larvae with amputated larvae

Anterior amputations show EdU incorporation near the amputation site. The initial pattern of EdU incorporation in anterior amputations (6 h post-amputation) is similar to the pattern observed in age-matched, uncut controls (Figure 3E,I). This pattern of EdU incorporation persists in animals 1 day post-amputation and in age-matched controls (Figure 3B,F,J). However, by 3 days postamputation, EdU+ cells are localized near the wound site in the anterior ectoderm and occasionally in the mesoderm of the amoutated animals (Figure 3G). EdU+ cells near the wound site persist through 5 days post-amputation in anterior ectoderm and mesoderm (Figure 3H). In contrast, there is a notable lack of EdU+ cells in the corresponding body region of unamputated animals (Figure 3C,D). The ratio of EdU+ cells to nuclei is higher in amputated animals at both 3 days post-amputation and 5 days post-amputation compared with the equivalent body region in uncut controls (Table 1). There is a significant difference between the number of EdU+ cells in the anterior body region anteriorly amputated larvae at 3 and 5 days postamputation when compared with age-matched, uncut controls (oneway ANOVA; Figure 3M).

Posterior amputations also show EdU incorporation localized near the wound site. In both cut and uncut larvae, the number of EdU+ cells decreases over time in the anterior and middle sections of the animal. Although the initial pattern of EdU incorporation in cells at 6 h post-amputation appears similar to that observed in Stage 6 uncut controls (Figure 3I), there is a progressive shift toward expression localized to the cut site in amputated larvae. Animals at 1 day post-amputation have fewer EdU+ cells in the anterior two-thirds of the body (Figure 3J) in comparison with uncut Stage 7 controls. By 3 days post-amputation, EdU incorporation is not detected through the anterior two-thirds of the body, and EdU+ cells are restricted to the area surrounding the cut site (Figure 3K). This localized pattern of EdU

incorporation persists through 5 days post-amputation (Figure 3L). Furthermore, cut larvae have more EdU+ cells in the posterior region than uncut controls (Table 2). The number of EdU+ cells in posterior sections of larvae at 3 and 5 days post-amputation is significantly higher compared with age-matched, uncut controls (one-way ANOVA; Figure 3N). Additionally, there is a higher ratio of EdU+ cells to Hoechst-stained nuclei localized at the wound site in posterior-amputated larvae relative to larvae with anterior amputations. Together, these data show a marked increase in cell proliferation at the wound site following both anterior and posterior amputations.

3.4 | Expression of the stem cell marker *vasa*

To further characterize the larval response to amputation, expression of the stem cell marker *vasa* was analyzed by in situ hybridization. In uncut larvae, *vasa* expression is dynamic from Stage 6 through Stage 9 (Dill & Seaver, 2008). In Stage 6 larvae, there was expression in the foregut, the mesoderm of the trunk, and the PGZ (Figure 4A). By Stage 8, expression was restricted to the foregut, the multipotent progenitor cell cluster (MPC), and the PGZ (Figure 4B). This pattern continued through Stage 9 (with some variability in detection of the MPC) (Figure 4C).

Expression of *vasa* transcript was detected at the wound site in both anterior and posterior amputations. Initially, the *vasa* expression pattern in both amputation groups was very similar to the observed pattern in uncut controls (6 h post-amputation; Figure 4D). However, by 2 days post-amputation, there was de novo expression in the anterior ectoderm at the amputation site of anteriorly cut larvae (Figure 4E). By 5 days post-amputation, expression at the wound site was no longer detected, although expression in the MPC and PGZ persisted (Figure 4F). In posterior amputations at 2 h post-amputation, trunk mesodermal expression was continuous from one side of the animal to the other and wrapped around the posterior end of the body (Figure 4G). We interpret this expression along the posterior face of the animal to be the result of wound healing that pulled the two lateral trunk domains of expression together. At 2 days post-

TABLE 1 Mean number of EdU+ cells, Hoechst-stained nuclei, and ratio of EdU+ cells to Hoechst-stained nuclei in three body sections following anterior amputation.

		Body section						
			Anterior		Middle		Posterior	
Time	Stain	Uncut	Cut	Uncut	Cut	Uncut	Cut	
6 h	# EdU+	133	102	466	235	387	136	
	# Hoechst	418	392	1216	417	551	250	
	Ratio	0.32	0.26	0.38	0.56	0.70	0.54	
3 days	# EdU+	3	29	18	2	14	24	
	# Hoechst	447	363	856	457	413	185	
	Ratio	0.01	0.08	0.02	0.00	0.03	0.13	
5 days	# EdU $+$	3	28	18	5	14	10	
	# Hoechst	147	359	856	516	413	219	
	Ratio	0.02	0.08	0.02	0.01	0.03	0.05	

		Body section					
		Anterior		Middle		Posterior	
Time	Stain	Uncut	Cut	Uncut	Cut	Uncut	Cut
6 h	# EdU+	133	70	466	217	387	225
	# Hoechst	418	155	1216	556	551	463
	Ratio	0.32	0.45	0.38	0.39	0.70	0.49
3 days	# EdU+	3	2	18	6	14	78
	# Hoechst	447	306	856	702	413	525
	Ratio	0.01	0.01	0.02	0.01	0.03	0.15
5 days	# EdU+	3	0	18	0	14	51
	# Hoechst	147	331	856	547	413	513
	Ratio	0.02	0.00	0.02	0.00	0.03	0.10

TABLE 2 Mean number of EdU+, Hoechst-stained nuclei, and ratio of EdU + cells to Hoechst-stained nuclei in three body sections following posterior amputation.

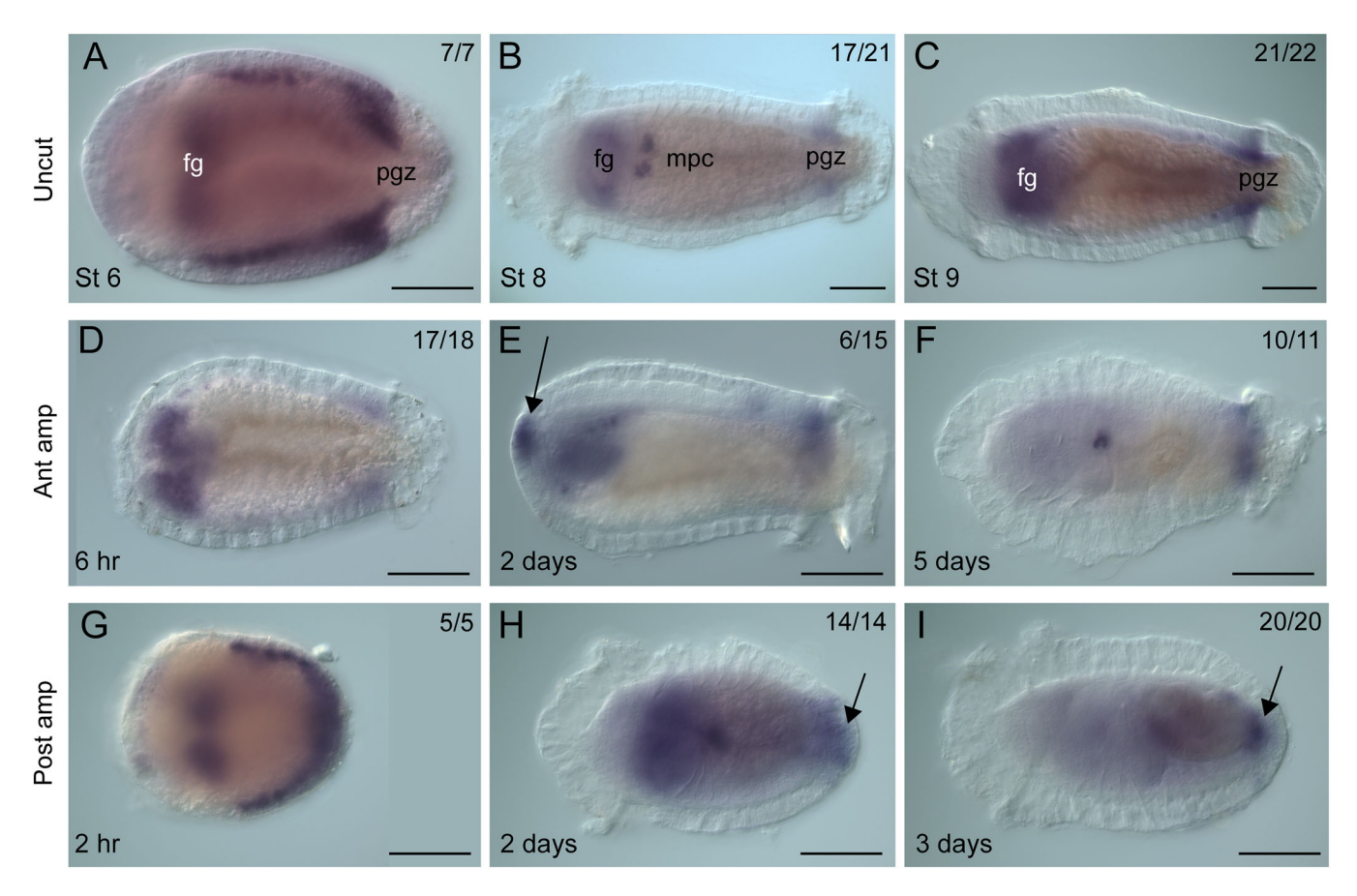


FIGURE 4 Expression of vasa at the wound site in amputated larvae of Capitella teleta. All images are oriented in ventral view with anterior to the left. The purple coloration indicates localization of vasa transcripts by in situ hybridization. (A–C) Patterns of vasa expression in uncut larvae at Stages 6, 8, and 9. (D–F) Larvae with anterior amputations at 6 h, 2 days, and 5 days post-amputation. De novo expression is observed in anterior amputations at 2 days post-amputation (E), as indicated by the arrow, and is no longer detectable by 5 days post-amputation (F). (G–I) Larvae with posterior amputations at 2 h, 2 days, and 5 days post-amputation. In posterior amputations, expression near the wound site is observed at both 2 days post-amputation (H) and 3 days post-amputation (I), as indicated by arrows. The number of animals scored that resembled the image shown (out of the total number of animals examined) is noted in the top right corner. Scale bars = $50 \mu m$. Ant amp, anterior amputation; fg, foregut; mpc, multi-progenitor cell cluster; post amp, posterior amputation; pgz, posterior growth zone.

amputation, *vasa* was expressed in the posterior mesoderm and ectoderm near the wound site (Figure 4H). This expression near the wound site was also detectable 3 days post-amputation (Figure 4I)

and 4 days post-amputation (data not shown). In summary, *vasa* expression was detected at the wound site 2 days post-amputation for both anterior and posterior amputations.

3.5 | Generation of new tissue

The presence of localized cell proliferation at the wound site (Figure 3G,H,K,L) and at what appeared to be growth of new tissue (Figure 2E) warranted a more detailed investigation of the tissue surrounding the wound site. To distinguish between preexisting tissue and new tissue, the location of the cut site was determined using the nervous system and musculature markers. We used a framework commonly used for identifying the cut site in juvenile worms with an antiacetylated tubulin antibody marking the nervous system (Figure 1B). An abrupt change in the thickness of the connective nerves was used to indicate the position of the cut site (Figure 1D; Figure 5B,B',C). An abrupt decrease in the density of muscle fibers also indicated the location of the cut site (Figure 1E; Figure 5F,F'). Typically, there was a precise concordance in position between an abrupt change in muscle fiber density and thickness of connective nerves. Therefore, we could consistently identify the location of the cut site using these two markers.

The identification of the cut site in amputated larvae allowed us to identify new tissue and quantify tissue distal to the amputation site. No evidence of significant growth of tissue was detected in anterior amputations between 6 h post-amputation and 3 days postamputation (see Table 3). In contrast, there was significant growth in posterior amputations between 6 h post-amputation and 5 days postamputation. Additional measurements of posterior amputations indicated a significant change in body width (body width at the mouth compared with immediately posterior to the cut site) between 6 h post-amputation and 5 days post-amputation. This information is consistent with the presence of new growth in posterior amputations; regenerated tissue is often more narrow than the width of the original tissue. Although the position of the cut site, as identified by muscle and nerve markers, indicated new growth, there was one measurement that did not. Measurements from the posterior end of the pigmented gut to the posterior of the animal for both larvae 5 days post-amputation and Stage 9 larvae 6 h post-amputation did not show a significant difference between these two groups.

We next characterized the nervous system and musculature of the tissue distal to the cut site. Similar to what was observed in control larvae 6 h post-amputation (Figure 5D), anterior amputations in larvae 3 days post-amputation lacked clear evidence of neurites and muscle fibers distal to the wound site (Figure 5E-E''). posteriorly amputated larvae, a mixture of results was observed. In posteriorly amputated larvae with a discernable cut site and new growth, neuronal projections distal to the amputation site were observed 2 days post-amputation, but not at 6 h post-amputation (Figure 5B,F-F"). There were also cases in which there was seemingly no change in the larval nervous system (165/395; Figure 5G). Cases in which new growth was not observed lend confidence to those instances when we observed processes distal to the cut site (compare Figure 5F" and G). At 5 days post-amputation, nerve processes persisted in tissue distal to the cut site (Figure 5H,H'). These longitudinal nerve processes were located at the midline and spanned the length of the new tissue. Additionally, there were circumferential processes similar to the orientation of peripheral nerves, although these

processes were somewhat disorganized relative to peripheral nerves in uncut animals (Figure 5H'). These neuronal processes were oriented medial to lateral, extending from the midline. The entire region of the new tissue had a lower density of muscle fibers relative to the preexisting tissue (Figure 5B,H'). The muscle fibers that were present were predominately longitudinal muscle fibers. In many cases, individual longitudinal muscle fibers appeared to extend from preexisting tissue into tissue distal to the amputation site (Figure 5H", arrow), whereas circular muscle fibers were only occasionally observed posterior to the amputation site. These circular fibers were unlikely to be associated with a telotroch because amputated larvae lacked evidence of regrown ciliary bands. A similar arrangement of muscle and nerve fibers in the tissue distal to the amputation site was present in animals 7 days post-amputation (data not shown). Although we observed multiple tissue types distal to the cut site, we did not observe evidence of new segments. Conventionally, newly formed segments are characterized by the appearance of new ganglia, regularly spaced circumferential peripheral nerves, and segmental boundaries. The nervous system distal to the cut site had not organized into ganglia by 7 days postamputation, and peripheral nerves were disorganized. We did not observe segmental boundaries in the ectoderm. In conclusion, new tissue growth was observed along with changes in organization of the nervous system and musculature in posteriorly amputated larvae, although there was a lack of new tissue in anteriorly amputated larvae.

3.6 Neural specification and differentiation

Next, we sought to determine whether the neural and muscle cell types observed distal to the amputation site resulted from the birth of new cells. We rationalized that expression of molecular markers of cell fate specification and differentiation in the tissue distal to the amputation site indicated birth of new cells. For the nervous system, gene expression patterns of neural specification (ash1) and neural differentiation markers (elav) were analyzed near the wound site (Meyer & Seaver, 2009). In C. teleta, ash1 is a marker of neural specification during initial neurogenesis of the brain and VNC (Meyer & Seaver, 2009; Sur et al., 2017). In Stage 6 larvae, ash1 was expressed in the brain, foregut, ventral neural ectoderm, PGZ, and the mesoderm in the pygidium (Figure 6A). By Stage 9, ash1 expression was restricted to the foregut and PGZ (Figure 6B). In anterior amputations, the pattern observed at 6 h post-amputation for ash1 expression mirrored that of uncut Stage 6 larvae, with the notable exception of missing brain expression due to the removal of the head (Figure 6C). In specimens 3 days post-amputation, ash1 was expressed in both the anterior ectoderm and pharynx (Figure 6D). Expression in the ectoderm could be regarded as de novo ash1 anterior expression because agematched, uncut controls lacked anterior ectoderm expression (32/39; compare panels Figure 6B and D,E) The novel anterior ectodermal expression of ash1 at 3 days post-amputation was present in a punctate pattern similar to the pattern observed in the anterior ectoderm during C. teleta brain development. In contrast, expression in the

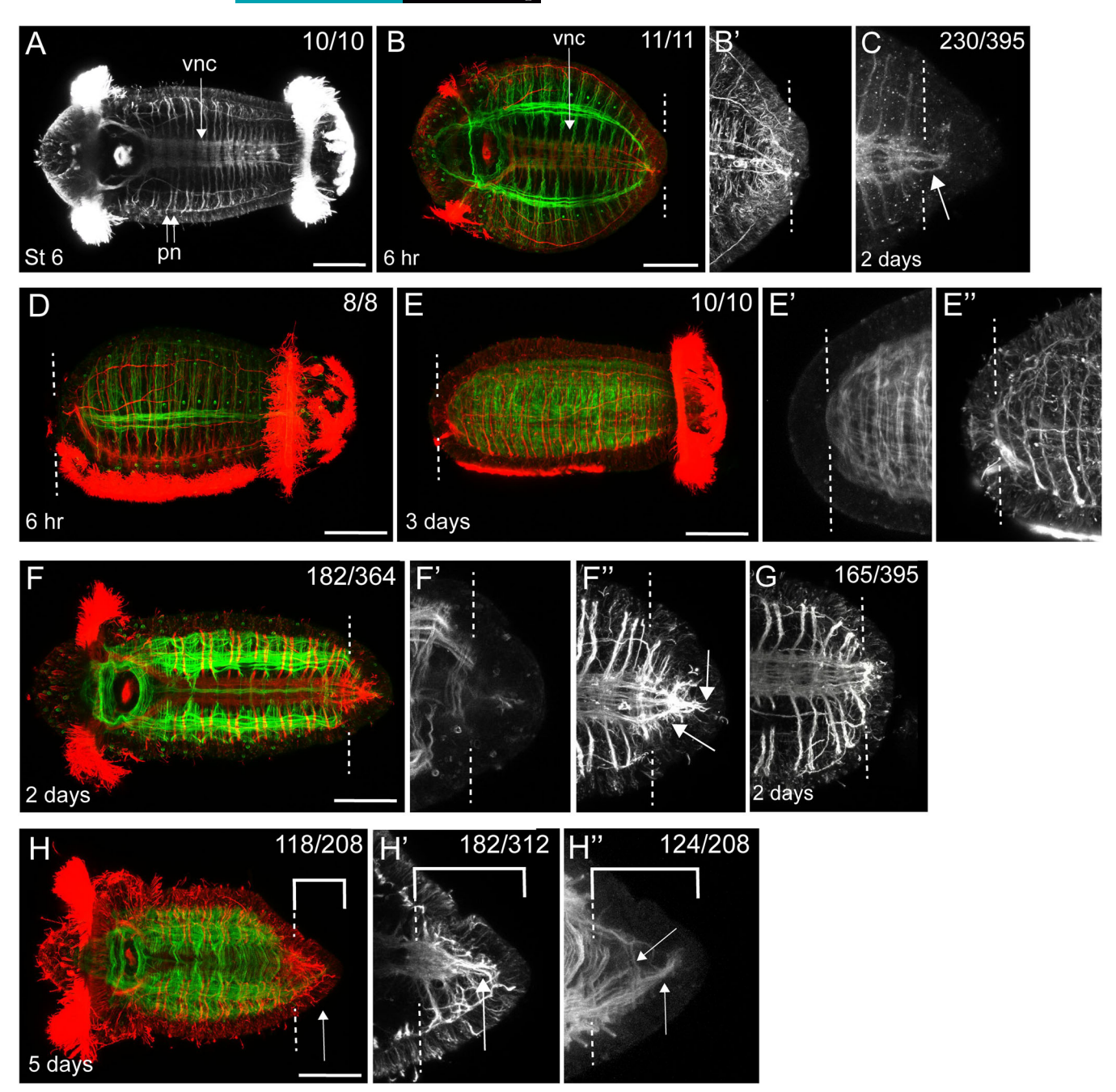


FIGURE 5 Tissue response to amputation in larvae of *Capitella teleta*. (A–C) and (F–H") are oriented in ventral view. (D–E") are oriented in lateral view. In all images, anterior is to the left. Color images (B, D, E, F, and H) show larvae labeled with anti-acetylated tubulin (red) and phalloidin (green) to indicate the nervous system and musculature. Larvae shown in panels (A, B', C, E", F", G, and H') are labeled with anti-acetylated tubulin. Larvae in panels (E', F', and H") are stained with phalloidin. (A) Uncut Stage 6 larva labeled with anti-acetylated tubulin to visualize the nervous system and ciliary bands. (B, B') The same specimen, 6 h post-amputation. (C) Neural fibers (arrow) are present distal to the cut site in a posterior amputee 2 days post-amputation. (D) Larva 6 h after anterior amputation. (E–E") are the same specimen, 3 days after anterior amputation. (E') Magnified view of muscle fibers at the cut site. (E") Magnified view of the nervous system at the cut site. (F–F") are the same specimen, 2 days post-amputation. (F) Nervous system and musculature in a larva 2 days post-amputation. (F') Magnified view of posterior wound site showing few muscle fibers distal to cut site (F") Magnified view of posterior wound site showing neuronal fibers in the tissue distal to the amputation site (arrows). (G) Specimen lacking neural fibers distal to the cut site. (H–H") are the same specimen, 5 days after posterior amputation. (H') Neurites distal to the cut site (arrow) (H") Longitudinal and circular muscles are present distal to the cut site (bracket). White brackets in (H–H") indicate tissue distal to the amputation site. Amputation sites are indicated by white dotted lines. The number of animals scored that resembled the image shown (out of the total number of animals examined) is noted in the top right corner. Scale bars = 50 μ m. vnc, ventral nerve cord; pn, peripheral nerves.

TABLE 3 Mean lengths of tissue distal to the cut site, and ratio of body width at the mouth: body width at the cut site for posteriorly amputated larvae.

		Measurement			
Amputation site	Time point	Muscle	Nervous system	Gut	Body width ratio
Anterior	6 h	19 μm	18 μm	N/A	N/A
	3 days	22 μm	15 μm	N/A	N/A
		t = 1.12 $p = 0.275$	t = 1.45 $p = 0.165$	N/A	N/A
Posterior	6 h	17 μm	12 μm	N/A	0.675
	5 days	62 μm	67 μm	-	0.453
		t = 3.78 $p = 0.00178$	t = 4.93 $p = 0.000179$	N/A	t = 9.03 $p < 0.00001$
	6 h (Stage 9)	N/A	N/A	37 μm	N/A
	5 days	N/A	N/A	45 μm	N/A
				t = 1.03 $p = 0.315$	

Note: Statistical tests indicate differences between means for amputated larvae compared with 6-h controls. N/A, not measured.

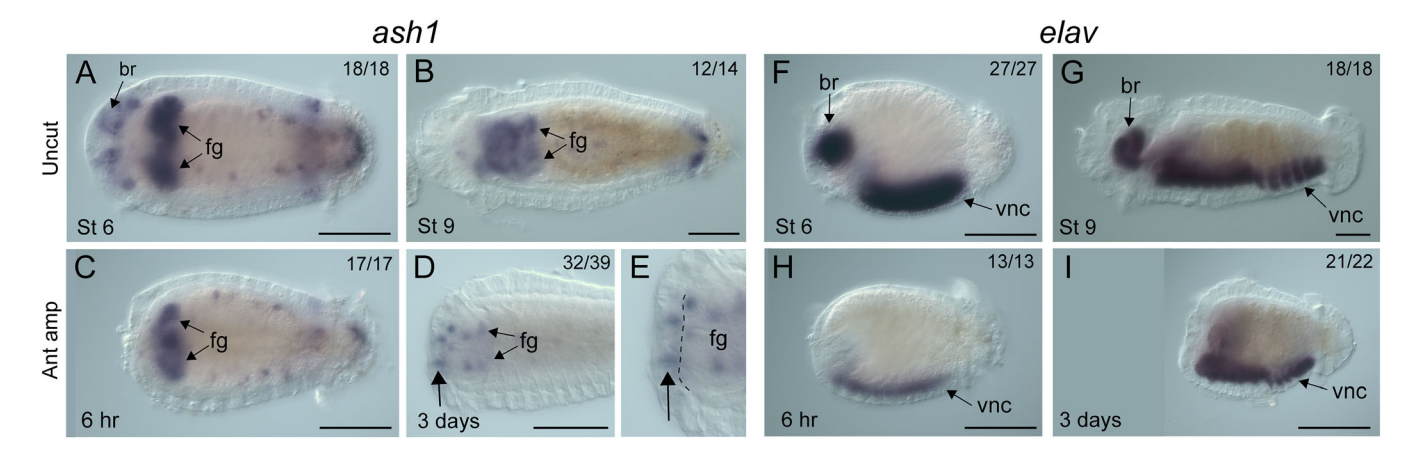


FIGURE 6 Amputation induces ash1 but not elav expression at the anterior wound site in larvae of Capitella teleta. All images are oriented with anterior to the left. Panels (A–E) are ventral views and (F–I) are lateral views. The purple coloration indicates expression of either ash1 (A–E) or elav (F–I) transcripts. Panels (C–E) and (H, I) are anterior amputations. (A) Stage 6 larva, uncut control. (B) Stage 9 larva, uncut control. (C) 6 h post-amputation. (D, E) These images show the same individual, 3 days post-amputation. Vertical arrows indicate novel ash1 ectodermal expression. The boundary between ectodermal and mesodermal layers is indicated by a black dotted line. (F) Stage 6 larva, uncut control. (G) Stage 9 larva, uncut control. (H) 6 h post-amputation. (I) 3 days post-amputation. The number of animals scored that resembled the image shown (out of the total number of animals examined) is noted in the top right corner. Scale bars $= 50 \, \mu m$. Ant amp, anterior amputation; br, brain; fg, foregut; vnc, ventral nerve cord.

pharynx corresponded with expression in age-matched uncut controls, albeit with fewer cells.

After observing novel anterior neural specification following amputation, the next step of neurogenesis was analyzed by characterizing the expression pattern of *elav*, a marker of differentiating neurons. Between Stages 6 and 9 in uncut controls, *elav* was expressed in the brain and the VNC (Figure 6F,G). In larvae with anterior amputations 6 h post-amputation, *elav* was expressed only in the VNC (Figure 6H). This expression pattern persisted through 3 days post-amputation, with no new expression domains observed in amputated animals (21/22; Figure 6I). In the one differing case of the 22 scored

animals, there were a few *elav*-expressing cells in the anterior ectoderm. These cells were part of the pharynx that abnormally everted during morphogenesis.

3.7 | Amputation induces expansion of *MyoD* expression

We also examined the expression of *MyoD*, a gene known for its role in muscle specification and differentiation (Zammit, 2017). In uncut larvae, *MyoD* was expressed in the mesoderm of the posterior trunk segments

at Stage 6 (Figure 7A) and Stage 9 (Figure 7B). There is a developmental progression from anterior to posterior in the larval trunk, with the more mature segments having an anterior position (Seaver et al., 2005). Thus, MyoD was expressed in the younger and newly forming segments. Six hours after both anterior and posterior amputations (6 h post-amputation), expression was restricted to the posterior portion of the trunk (Figure 7C,E), similar to what was observed in uncut controls. At 7 days post-amputation in anterior amputees (Figure 7D) and at 3 days post-amputation in posterior amputees (Figure 7F), there was a drastic expansion of MyoD mesodermal expression along the entire length of the

trunk. This expansion in *MyoD* expression was in preexisting tissue in older segments and included tissue distant from the wound site in the case of posterior amputations.

3.8 Rare regeneration of differentiated cell types

Following amputations, a few differentiated cell types occasionally regenerated, namely the larval eyes and cilia. Larvae have two cerebral eyes, with each eye consisting of three cells: a pigment cell

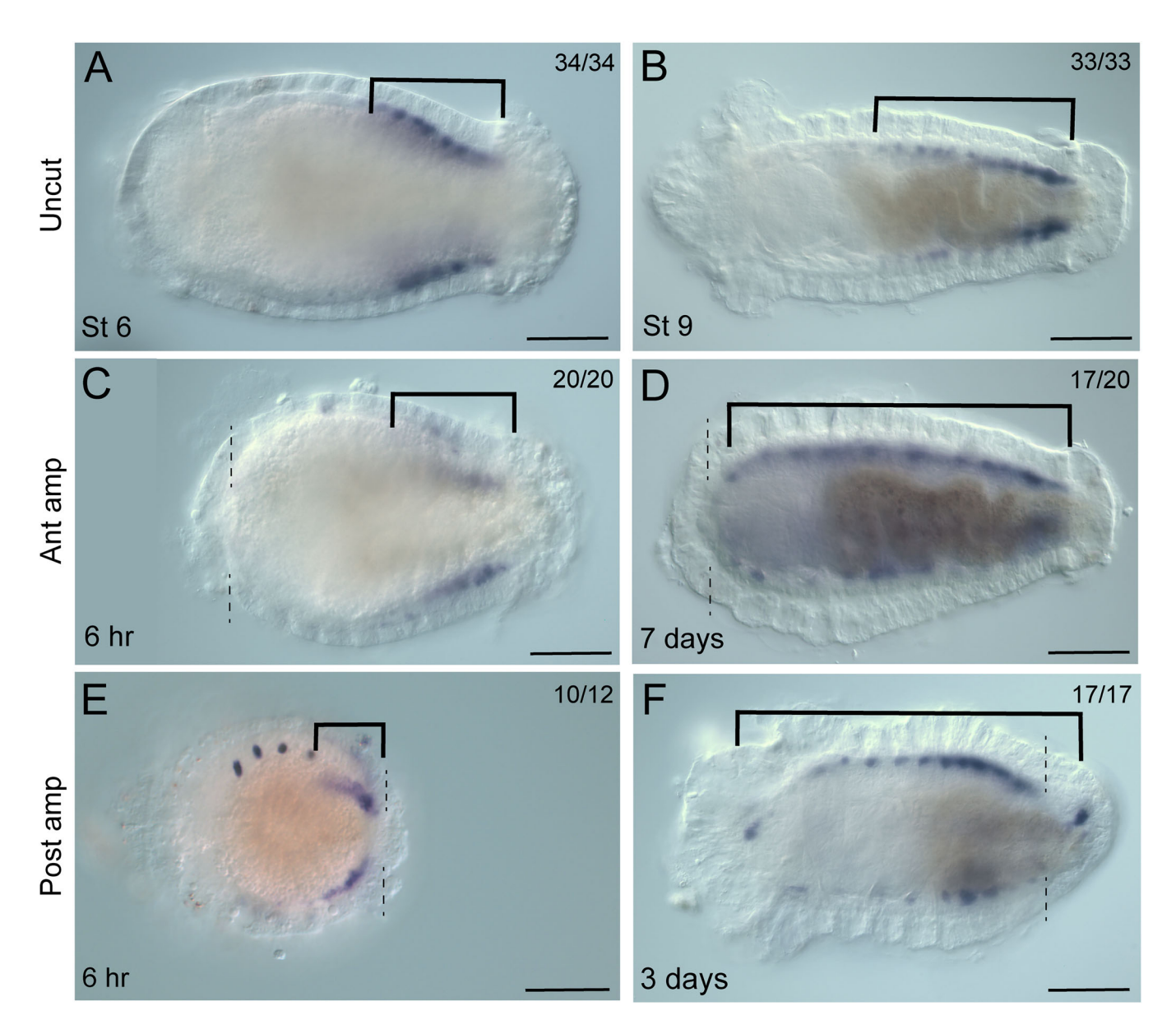


FIGURE 7 Amputation induces expansion of *MyoD* expression in larvae of *Capitella teleta*. All images are oriented in ventral view with anterior to the left. Localization of *MyoD* transcripts is visualized by the purple coloration. (A) Stage 6 larva, uncut control. (B) Stage 9 larva, uncut control. *MyoD* is expressed in the posterior trunk mesoderm. (C) 6 h after anterior amputation. (D) Anterior shift of anterior boundary of *MyoD* expression is observed at 7 days after anterior amputation. (E) 6 h after posterior amputation. Spots of staining anterior to the bracket is nonspecific trapping in the chaetae. (F) *MyoD* is expressed along the length of the body in animals 3 days post-amputation (compare with E). Brackets indicate the regions of detectable *MyoD* expression along the anterior–posterior axis. Amputation sites are indicated by black dotted lines. The number of animals scored that resembled the image shown (out of the total number of animals examined) is noted in the top right corner. Ant amp, anterior amputation; post amp, posterior amputation. Scale bars = 50 µm.

(Figure 8A), a sensory cell (Figure 8C), and a support cell (Yamaguchi & Seaver, 2013). The pigment cell is readily distinguished by its orange pigment granules, and the sensory cell can be visualized by immunolabeling with the antibody 22C10 (Yamaguchi & Seaver, 2013). We were unable to assess the presence of the support cell. In uncut Stage 9 larvae, the pigment cells were located slightly anterior, if not inline, with the prototroch, in a lateral position (Figure 8A). The sensory cell in uncut Stage 9 larvae (Figure 8C) was located immediately adjacent and lateral to the pigment cell and had an axonal projection extending from the cell body to the external surface of the ectodermal epithelium. The pigment and sensory cells were scored as independent characters. Following head amputation, a few pigment cells regenerated, and they were variable in location and number (28/420; 3-5 days post-amputation). Additionally, the pigment cells in amputated larvae were ectopically positioned. For example, as seen in Figure 8B, there was a pigment cell in proximity to the midgut. Regenerated sensory cells were also observed in amputated larvae and also exhibited variability in location (8/220, 3-7 days post-amputation). Axon projections in regenerated sensory cells extended to the outer ectodermal surface of the animals (Figure 8D). There was a higher percentage of cases with regenerated pigment cells (7%) compared with sensory cells (4%) in anterior amputations (Table 4). Summation of the total number of pigment cells and sensory cells indicates that at least one cell of the eye regenerated in 6% of the amputated larvae (36/640).

We were surprised by the appearance of new larval eye cells in amputated larvae of C. teleta because regeneration of anterior structures is not reported in adults (Yamaguchi & Seaver, 2013). Therefore, we conducted a similar experiment with juveniles. Four-week-old juveniles were amputated immediately anterior to the mouth, with removal of the eye cells. After screening for successful wound healing and visual inspection to ensure that pigment cells were removed, a subset of the amputated juveniles was fixed at 4 h post-amputation to confirm the removal of the sensory cells (21/21). No pigment cells were observed in amputated juveniles at 7 days post-amputation (0/43). However, a small proportion of cases with eye sensory cells were observed (14%, [6/43]; Figure 8E). Regenerated sensory cells were ectopically located (compare Figure 8E,F). Five of the six juveniles with regenerated sensory cells had a small portion of brain present in the anterior of the animal; only one juvenile had a sensory cell in the absence of a brain. In summary, pigment cells did not regenerate in juveniles, although sensory cells were detected in a small fraction of cases. These rare instances of eye sensory cell regeneration

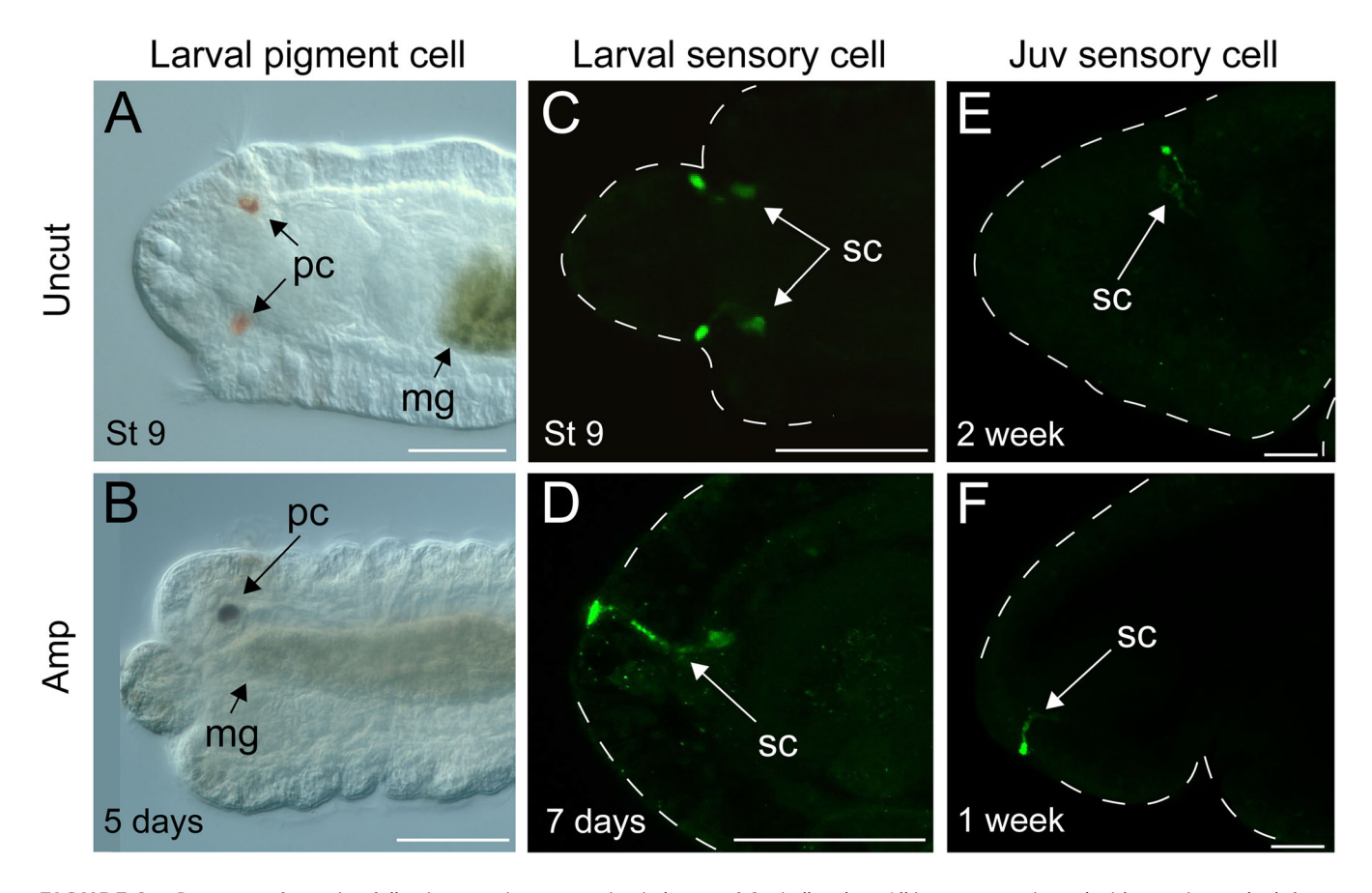


FIGURE 8 Rare eye reformation following anterior amputation in larvae of *Capitella teleta*. All images are oriented with anterior to the left. Panels (A–D) are ventral views. (A) DIC image of the anterior end of an uncut Stage 9 larva. (B) DIC image of the anterior end of a larva 5 days after anterior amputation. The image shown is a merge of multiple focal planes. The pigmented cells of the eye are indicated by arrows. (C–F) Eye sensory cells, labeled by the 22C10 antibody (green). (C) Uncut Stage 9 larva, control. (D) Anteriorly amputated larva, 7 days post-amputation. (E, F) are juvenile worms in lateral view. (E) Uncut 2-week-old juvenile. (F) Juvenile 1 week post-amputation of the head. The dotted line indicates the outline of the animal. Scale bars $= 50 \mu m$. Juv, juvenile; mg, midgut; pc, pigment cells; sc, sensory cells.

TABLE 4 Number of pigment eye cells, sensory eye cells, and total number of eye cells, where at least one pigment or sensory cell was observed, in anteriorly amputated larvae at 6 h post-amputation and 3–7 days post-amputation.

Time post-amputation	Pigment eye cell (%)	Sensory eye cell (%)	${\bf Pigment + sensory \ cells \ (\%)}$
6 h	0/46 (0)	0/31 (0)	0/57 (0)
3-7 days	28/420 (7)	8/220 (4)	36/420 (6)

represented the most dramatic phenotype observed following juvenile anterior amputations.

There are four external ciliated structures in larvae of C. teleta: prototroch, neurotroch, telotroch, and cilia of the pygidium (Figure 9A,B). The prototroch and telotroch are composed of relatively long cilia (prototroch cilia length \sim 25–30 μ m, telotroch cilia length \sim 20–28 µm), and the neurotroch and pygidium have short cilia (neurotroch cilia length \sim 8-10 µm, pygidium length \sim 5-7 µm). At 6 h post-amputation, larvae lacked long cilia at the cut site (Figure 9C,D) because of amputation of the prototroch and telotroch in anterior and posterior amputations, respectively. At 5 days post-amputation, short cilia (~8 µm in length) were observed in rare cases (7%, 12/161) at the anterior end of anteriorly cut animals, distal to the amputation site (compare Figure 9C,E,G). Long cilia were not observed following anterior amputations (0/161). Although rare (6%, 22/370), both long (\sim 25 μm) and short (\sim 9 μm) cilia appeared distal to the cut site 3-7 days after posterior amputations (compare Figure 9D,F with Figure 9H,H').

3.9 | Metamorphosis following amputation

In C. teleta, larvae at Stage 9 are competent and can be induced to undergo metamorphosis into juveniles (Burns et al., 2014). Following amputation, larvae were screened for stereotypical signs of successful settlement and metamorphosis following the definition of Cohen and Pechenik (1999). These changes include a loss of swimming and initiation of burrowing behavior, loss of both ciliary bands (telotroch and prototroch), and the appearance of an elongated, worm-like body shape. Uncut, uninduced control larvae swam with their prototroch and telotroch bands intact for the duration of the experiment (2 h, 532/534; Figure 10A). In contrast, virtually all larvae in the induced, unamputated control group successfully underwent metamorphosis within 2 h of exposure to the metamorphic cue and settled on the bottom of the dish, dropped their cilia, adopted burrowing behavior, and extended in length along the anterior-posterior axis (203/207; Figure 10B). Both sets of amputated larvae followed a similar pattern to what was observed in unamputated larvae. Specifically, 1 day after anterior amputation, larvae either continued to swim in the water column in the absence of a metamorphic cue (65/66; Figure 10C) or settled to the bottom of the dish and underwent metamorphosis within 2 h of exposure to a metamorphic cue (135/136; Figure 10D). Similarly, individuals whose posterior ends had been removed retained their prototrochal bands and continued to swim in the absence of a metamorphic cue (65/65; Figure 10E, arrow), yet underwent rapid

settlement and metamorphosis within 2 h of exposure (143/144; Figure 10F). In the absence of an induction cue, amputated larvae continued to swim in the water column and retained their ciliary bands for several days, which demonstrated that amputation itself did not induce metamorphosis (Figure 10C,E). Together, these results demonstrate that larvae of *C. teleta* can detect a metamorphic cue and successfully execute metamorphosis in the absence of either anterior or posterior structures.

4 | DISCUSSION

4.1 | Limited regeneration in larvae of *C. teleta*

This study demonstrates that the initial events in response to amputation appear to be quite similar between larvae and juveniles of C. teleta. Following both anterior and posterior amputation, larvae wound heal in a similar time frame as previously reported for posterior amputation of juveniles (i.e., within 6 h post-amputation; de Jong & Seaver, 2016). Following wound healing, EdU+ cells appear localized at the wound site at 2 days post-amputation during posterior regeneration in iuveniles, and the number of EdU+ cells increases over time (de Jong & Seaver, 2016). EdU incorporation in anterior-facing wound sites in juveniles of C. teleta has not been formally characterized. In both anterior and posterior amputations in larvae, EdU is incorporated near the wound site by 3 days post-amputation and this persists through 5 days post-amputation, comparable to the pattern of EdU incorporation at the wound site in regenerating juveniles. There is a difference in the number of EdU+ cells between anterior and posterior amputations in larvae, with posterior amputations exhibiting more EdU+ cells. One difference in cell proliferation patterns between juveniles and larvae is a change in position of the localized EdU+ cells. During posterior regeneration in juveniles, localization of EdU+ cells progressively shifts anteriorly to a subterminal position, a shift that corresponds with the re-establishment of the juvenile PGZ. We did not observe such a shift in larvae. It is interesting to note that in adults of the annelid Paranais litoralis, BrdU is incorporated near the anterior wound site even though these animals have lost the ability to regenerate their heads (Bely & Sikes, 2010). This finding, along with our results in larvae of C. teleta, emphasizes that a block in regeneration can occur subsequent to the initiation of cell division at the wound site, and cell division at the wound site is not a reliable predictor of successful regeneration.

Interestingly, expression of the stem cell marker vasa at the wound site was observed in both anteriorly and posteriorly amputated

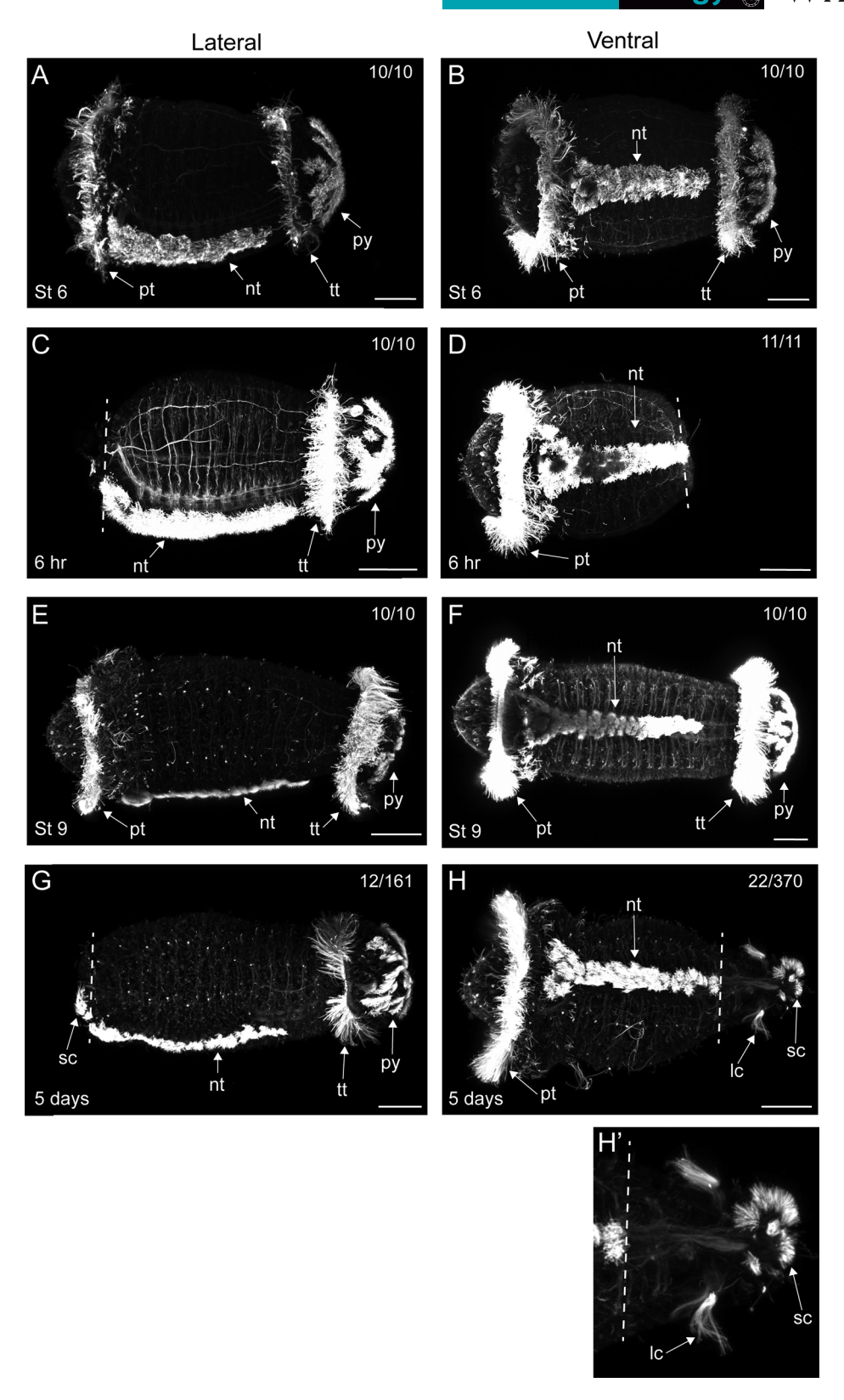


FIGURE 9 Rare re-formation of cilia occurs in amputated larvae of *Capitella teleta*. Animals are labeled with anti-acetylated tubulin (white). All images are oriented with anterior to the left. Panels (A, C, E, G) are in lateral view, panels (B, D, F, H, H') are in ventral view. (A, B) Uncut Stage 6 larva. (C) Anteriorly amputated larva 6 h post amputation. (D) Posteriorly amputated larva 6 h post amputation. (E, F) Uncut Stage 9 larva. (G) Anteriorly amputated larva 5 days post amputation. (H, H') Larva 5 days post-amputation, with both long cilia and short cilia distal to the cut site (arrows). H' is a magnification of H. The number of animals scored that resembled the image shown (out of the total number of animals examined) is noted in the top right corner. Amputation site is indicated by the white dotted line. Scale bars = 50 µm. Ant amp, anterior amputation; lc, long cilia; nt, neurotroch; post amp, posterior amputation; pt, prototroch; pyg, pygidium; sc, short cilia; tt, telotroch.

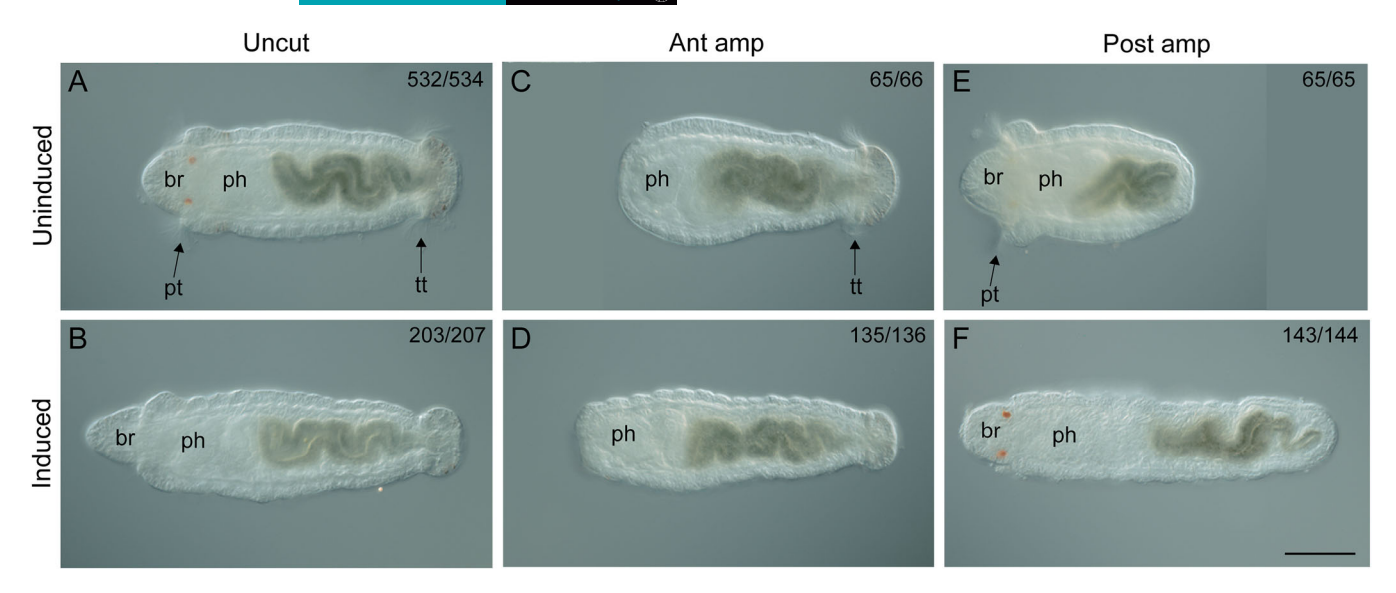


FIGURE 10 Induction of metamorphosis in amputated larvae of *Capitella teleta*. All images are oriented in ventral view with anterior to the left. (A) Uncut Stage 9 larva. (B) Uncut larva 2 h after induction with metamorphic cue. (C) Anteriorly amputated larva not exposed to metamorphic cue. (D) Anteriorly amputated larva 2 h after exposure to metamorphic cue. (E) Posteriorly amputated larva not exposed to metamorphic cue. (F) Posteriorly amputated larva 2 h after exposure to metamorphic cue. The number of animals scored that resembled the image shown (out of the total number of animals examined) is noted in the top right corner. All images have the same magnification; scale bar = 50 μm. Ant amp, anterior amputation; br, brain; ph, pharynx; post amp, posterior amputation; pt, prototroch; tt, telotroch.

larvae. In successful posteriorly regenerating juveniles, vasa is expressed locally at the wound site at 2 days post-amputation and persists for several days (de Jong & Seaver, 2017). In larvae, the duration of vasa expression and proportion of vasa-positive cases is different between anterior and posterior amputations. In anterior amputations, vasa is expressed in the anterior ectoderm in approximately one third of cases and is transient, detectable at 2 days postamputation but not 5 days post-amputation. Conversely, localized vasa expression is observed at 2 days post-amputation and persists through 5 days post-amputation in posterior amputations. We interpret the localized expression of vasa at the posterior wound site as either the result of de novo expression or expression maintained from an earlier stage (i.e., 6 h post-amputation). The spatial and temporal patterns of EdU incorporation and vasa expression are very similar in posterior amputations. In contrast, vasa expression has a shorter duration than EdU incorporation near the wound site in anterior amputations. We hypothesize that these differences between anterior and posterior amputations is related to the new tissue growth in posterior amputations that is absent following anterior amputations.

Additional features of juvenile posterior regeneration are the presence of neural projections into the wound site and muscle reorganization distal to the amputation site. In juveniles, this phenomenon is observed at \sim 2 days post-amputation (de Jong & Seaver, 2016). In larvae with posterior amputation, neurites are present distal to the cut site by 2 days post-amputation. However, these neurites were not observed in larval anterior amputations. With respect to muscle fiber organization, there is an abrupt transition between the presence and absence of muscle fibers distal to the cut site in posterior amputations in both juveniles and larvae that was not observed in anterior amputations in larvae. We were unable to determine whether fibers present distal to the amputation site in

posterior amputations of larvae resulted from birth of new neural or muscle cells or from the extension of preexisting cells.

To better understand the characteristics and development of the tissue distal to the cut site in larvae, we characterized the specification and differentiation of cell types (i.e., neural cell types and cilia) in amputated larvae. The timing of neural specification or differentiation in juvenile regeneration has not been investigated in detail, but differentiated tissues are present by 7 days post-amputation (de Jong & Seaver, 2016). Analysis of de novo ash1 expression indicates the specification of neural fates in larval anterior amputations. Surprisingly, subsequent differentiation of neural tissues was not detectable, as illustrated by the absence of elav expression in larval amputations. Anterior amputation of larvae results in incomplete tissue and structure regeneration, which is an observation consistent with the response in juveniles to anterior amputations. Despite a general lack of anterior structural differentiation in amputated larvae, we surprisingly observed rare cases in which differentiated eye cells and cilia reappeared within 3-7 days post-amputation. Additionally, sensory eye cells (but not pigment cells) regenerated in juveniles at a higher proportion than in larvae (14% in juveniles, 4% in larvae). Although rare, the absence of eyes immediately following amputation and the ectopic location of the observed eye cells made us confident that these cells are regenerated eye cells in amputated larvae and juveniles. One possible explanation for the variation in cilia and eye cell regeneration across individuals is variance in maternal nutritional output.

In summary, the beginning stages of regeneration (i.e., wound healing, localized cellular proliferation, and expression of stem cell markers) occur in amputated larvae, but complete replacement of lost tissue or of cell or tissue differentiation does not occur. These data indicate that larvae of *C. teleta* exhibit limited regeneration abilities

relative to the successful posterior regeneration observed in juvenile and adult stages. Additionally, a lack of embryonic regulation and the detection of initial stages of regeneration in larvae suggest that in *C. teleta* there is a gradual transition in regenerative potential, rather than a stark change in potential that corresponds to metamorphosis.

4.2 | Amputation-induced expression in preexisting tissue

MyoD functions in muscle development, and its expression in muscle progenitor cells is an indication of myogenesis (Rawls & Olson, 1997; Zammit, 2017). In response to amputation, MyoD expression expands across the length of the larval body in C. teleta, far from the wound site. This expanded expression may result in an increase in muscle cell number to compensate for a decrease in body length following amputation, although we did not observe an obvious increase in the number of muscle fibers 3-5 days post-amputation. Alternatively, expanded expression of MyoD may be an injury-specific response that leads to cell dedifferentiation and return to a precursor state. Such a precursor cell population may contribute to regenerating tissue. It is notable that the induction of expanded MyoD expression occurs in the absence of a complete regeneration response. Regardless, future functional work is needed to better understand the implications of this change in MyoD expression in response to amputation. Changes in gene expression in response to amputation have previously been documented in C. teleta and other annelids (de Jong & Seaver, 2016; Kozin & Kostyuchenko, 2015; Pfeifer et al., 2012; Takeo et al., 2008). However, most examples documented to date are changes in expression of positional identity genes, and their new expression likely reflects repatterning of the body fragment in response to amputation.

4.3 | Metamorphosis following amputation

Amputated larvae of C. teleta undergo successful metamorphosis. We were surprised to observe metamorphosis following anterior amputations. In other spiralians, it has been hypothesized that the brain and other anterior sensory organs function in the detection and response to metamorphic cues (Chartier et al., 2018; Conzelmann et al., 2013; Hadfield, 2010; Hadfield et al., 2000). In C. teleta, chemosensitive ciliated cells in the head ectoderm were proposed to relay metamorphosis signals directly to the cerebral ganglia (Biggers & Laufer, 1999). More recently, a study hypothesized that the inductive signal for metamorphosis is detected by sensory neurons that innervate the dorsal pharyngeal pad of the pharynx (Biggers et al., 2012). If the metamorphic cue was detected by anterior neurons, we would expect that removing the head would prevent metamorphosis. However, our results demonstrate that the brain is not required for detecting the metamorphic cue or for undergoing metamorphosis in C. teleta, which supports the hypothesis that detection of metamorphic cues in C. teleta likely occurs in the pharynx. It was similarly demonstrated in the polychaete Hydroides elegans that apical sensory neurons are not necessary for

successful metamorphosis (Nedved et al., 2021), suggesting that the brain may not be necessary for metamorphosis in some annelids.

It is yet to be determined whether the amputations performed during larval stages have lasting effects on survival and growth following metamorphosis. In addition, it remains to be seen whether juveniles induced from posteriorly amputated larvae redevelop posterior growth zones, can generate additional segments, or are capable of posterior regeneration. Future studies could examine the regeneration potential of juveniles that result from posteriorly amputated larvae. Additionally, it could be interesting to determine whether juveniles induced from anterior amputated larvae are capable of posterior regeneration in the absence of a brain.

4.4 | Larval regeneration in marine invertebrates

The regenerative potential of an animal can vary significantly across its life stages. In the literature, larvae with reduced regenerative ability relative to adults are described as having "attempted" or "limited" regeneration (Vickery et al., 2001). Using this convention, we categorize larvae of *C. teleta* as having limited regeneration. Here, we show that in *C. teleta* regeneration ability varies over the life cycle and there are different regeneration abilities between larval and juvenile stages. To our knowledge, published studies characterizing larval regeneration abilities in other annelid larvae are scarce.

Other bilaterian taxa suffer from a similar dearth in sampling larval and immature stages for their regenerative abilities. Within Spiralia, larval regeneration has been examined in one nemertean species. Similar to annelids, nemertean adult regeneration is variable (Zattara et al., 2019; Zattara & Fernández-Alvarez, 2022), In early stage larvae of Maculaura alaskensis, there appears to be high regenerative potential, which progressively decreases with maturation until it stabilizes in adults capable of posterior regeneration (Hiebert & Maslakova, 2015). Younger larvae of M. alaskensis are five times more likely to regenerate than older larvae following amputation (Moss, 2018). In Ecdysozoa, the other protostome clade, regeneration ability is generally restricted to appendages, rather than along the main body axis (Brenneis et al., 2023). However, recent work shows that immature instars of the sea spider Pycnogonum litorale can regenerate the midgut and gonads as well as appendages following bisection. Adult counterparts of P. litorale cannot regenerate and do not even survive the amputations, suggesting that regeneration ability is restricted to the immature instar stages (Brenneis et al., 2023).

Deuterostome larvae have been better surveyed for regeneration ability and there are numerous documented examples. The hemichordate *Ptychodera flava* has the ability to repeatedly regenerate all body parts when cut transversely or decapitated as an adult (Humphreys et al., 2022). Although larvae of *P. flava* can regenerate along the main body axis, they do not regenerate as well as the adults. In addition, regeneration ability differs across the larval body. Specifically, ventral regions in larvae of *P. flava* regenerate better than dorsal regions and posterior segments regenerate better than anterior segments (Luttrell et al., 2018). The larval tail of the cephalochordate *Branchiostoma*

floridae regenerates multiple tissues faster than adults following similar amputations (Zou et al., 2021). Unlike larvae of other clades, echinoderm larvae have been widely surveyed for regenerative potential in all classes with documented adult whole-body regeneration abilities (Cary et al., 2019; Vickery et al., 2001). Asteroids and echinoid larvae, such as Patiria miniata, can regenerate completely, regardless of developmental stage, demonstrating a stable regenerative ability throughout life (Carnevali, 2006; Oulhen et al., 2016; Vickery et al., 2002). In crinoids, there appears a trend of increasing regenerative potential over developmental time. For example, crinoid larvae display limited ability to regenerate body parts, with early-stage larvae of Antedon bifida (= rosacea) regenerating more poorly than late-stage larvae (Carnevali, 2006). In contrast, adults can replace lost structures even when reduced to one fifth of the original body size (Carnevali, 2006). In summary, no clear trends of increasing or decreasing regeneration abilities across the life cycle emerge from regeneration studies either within or across taxa, which suggests that change in regeneration ability across the life cycle is a variable trait.

Although we cannot currently identify trends reflecting how regeneration abilities change between larval and adult stages from a phylogenetic perspective, we can consider the impact of life history factors. Factors such as feeding (de Jong & Seaver, 2016; Özpolat et al., 2016; Zattara & Bely, 2013), duration of larval stage, and sublethal predation (Schoeman & Simon, 2023; Stewart, 1998) may better correlate with the regenerative abilities observed in an individual species. Unlike larvae of C. teleta, larvae of M. alaskensis, P. flava, and P. miniata feed and display an ability to replace complex structures following amputation. Larvae of M. alaskensis and P. miniata can swim in the water column for weeks or months (Cary et al., 2019; Moss, 2018) and larvae of P. flava for up to 300 days (Luttrell et al., 2018). In contrast, larvae of C. teleta and the crinoid A. bifida (= rosacea) are nonfeeding (Vickery et al., 2001) and have a short larval period before undergoing metamorphosis. Larvae of C. teleta swim in the water column for hours to a few days, and larvae of some crinoids swim for up to 10 days before settlement (Nakano et al., 2003). It has been previously proposed that the longer an animal is in the water column and vulnerable to predation, the greater risk there is of sublethal injury (Vickery & McClinktock, 1998). Sublethal damage could act as an evolutionary pressure to select for a robust regenerative ability. To that end, there may not be a strong selective advantage for regeneration in non-feeding, short-lived, brood-dwelling larvae of species such as C. teleta.

4.5 | Future directions

This study demonstrates differences in regenerative ability across developmental stages in *Capitella teleta*. Future studies could investigate physiological, cellular, and molecular differences between larvae and juveniles in response to amputation. One such difference may relate to nutritional status. It has been demonstrated that the extent of regeneration in juveniles of *C. teleta* and other annelids can

fluctuate depending on nutrition intake (de Jong & Seaver, 2016; Zattara & Bely, 2013). Because larvae of C. teleta are non-feeding, limited energy resources may contribute to their regeneration limitations. This nutrition hypothesis could be tested by two separate approaches. In the first, cells with high yolk content could be deleted in early-stage embryos to reduce maternally contributed nutrition. Previous work demonstrated that such deletions result in morphologically normal, albeit smaller larvae (Pernet et al., 2012). These larvae would have a reduced nutritional supply and may exhibit a further reduction in regenerative potential to what was observed in this study. The second approach would involve investigating regeneration abilities in a different annelid with a feeding larval form. A feeding larva with more nutritional resources may exhibit full regenerative abilities following amputation. Additionally, an annelid with a longer larval period would have more time to completely regenerate lost tissue following amputation during the early larval period, while also continually feeding

The timing of cell maturation may also limit larval regeneration and explain differences between larval and juvenile regenerative abilities in C. teleta. An example of one such developmental constraint may be in the timing of stem cell maturation. A previous study proposed that stem cells travel from the multipotent progenitor cell (MPC) cluster to the wound site during juvenile regeneration (de Jong & Seaver, 2017). MPC cells in larvae may be immature, thereby preventing these stem cells from positively contributing to successful regeneration. Specifically, nascent stem cells may not be capable of self-renewal or migration, or of contributing to the blastema (Juliano et al., 2010). The number of cells in the MPC cluster does not increase during larval development (de Jong & Seaver, 2017), which suggests that these cells may be quiescent during this time. A heterotopic transplant of a mature MPC cluster from juveniles into larvae would test this hypothesis, and an increased regenerative ability in larvae following transplantation would be expected. Such experiments in C. teleta might lead to a better understanding of the role that development has on regeneration.

Future studies can characterize the regeneration ability of other annelid larvae, particularly for species in which adults have different regenerative potential than in C. teleta. A correlation between adult and larval regenerative potential within individual species may exist. For example, there may be anterior regenerative ability in larvae in a species capable of anterior regeneration as an adult. If this correlation the larvae of Chaetopterus variopedatus (Cuvier & Latreille, 1829) would be predicted to regenerate both anterior and posterior structures. Adults of C. variopedatus can regenerate anteriorly following amputations at segment 15 or more anterior, and can regenerate posteriorly following amputation at any segment (Berrill, 1928; Cuvier & Latreille, 1829). Extensive additional sampling is needed before we can meaningfully determine whether the pattern observed in C. teleta is representative of other annelids. Additional sampling across annelids will also provide insight as to the extent of variation in larval regeneration abilities, and whether larval regenerative ability is as common as adult regenerative ability.

Invertebrate Biology &-WILEY 21 of 23

AUTHOR CONTRIBUTIONS

Alicia A. Boyd and Elaine C. Seaver conceived and designed the experiments. Alicia A. Boyd performed the experiments. Alicia A. Boyd and Elaine C. Seaver analyzed the data. Elaine C. Seaver and Alicia A. Boyd contributed reagents, materials, and analysis tools. Alicia A. Boyd and Elaine C. Seaver wrote the paper.

ACKNOWLEDGMENTS

We thank Karina Dill for cloning the *C. teleta MyoD* gene and characterizing its larval expression pattern. We thank Brent Foster, Lauren Kunselman, and Katie Feerst for critical reading of the manuscript.

DATA AVAILABILITY STATEMENT

The data that support the findings of this study are available from the corresponding author upon reasonable request.

ORCID

Elaine C. Seaver https://orcid.org/0000-0002-5098-3899

REFERENCES

- Alvarado, A. S. (2000). Regeneration in the metazoans: Why does it happen? *BioEssays*, 22, 578–590. https://doi.org/10.1002/(SICI)1521-1878(200006)22:6
- Alwes, F., Enjolras, C., & Averof, M. (2016). Live imaging reveals the progenitors and cell dynamics of limb regeneration. *eLife*, 5, e19766. https://doi.org/10.7554/eLife.19766
- Bely, A. E. (2006). Distribution of segment regeneration ability in the *Annelida*. *Integrative and Comparative Biology*, 46(4), 508–518. https://doi.org/10.1093/icb/icj051
- Bely, A. E., & Sikes, J. M. (2010). Latent regeneration abilities persist following recent evolutionary loss in asexual annelids. *Proceedings of the National Academy of Sciences of the United States of America*, 107(4), 1464–1469. https://doi.org/10.1073/pnas.0907931107
- Berrill, N. J. (1928). Regeneration in the polychaet Chaetopterus variopedatus. Journal of Marine Biological Association of the United Kingdom, 15(1), 151–158. https://doi.org/10.1017/S0025315400055594
- Biggers, W. J., & Laufer, H. (1999). Settlement and metamorphosis of Capitella larvae induced by juvenile hormone-active compounds is mediated by protein kinase C and ion channels. The Biological Bulletin, 196(2), 187–198. https://doi.org/10.2307/1542564
- Biggers, W. J., Pires, A., Pechenik, J. A., Johns, E., Patel, P., Polson, T., & Polson, J. (2012). Inhibitors of nitric oxide synthase induce larval settlement and metamorphosis of the polychaete annelid *Capitella teleta*. *Invertebrate Reproduction and Development*, 56(1), 1–13. https://doi.org/10.1080/07924259.2011.588006
- Blake, J. A., Grassle, J. P., & Eckelbarger, K. J. (2009). Capitella teleta, a new species designation for the opportunistic and experimental Capitella sp. I, with a review of the literature for confirmed records. Zoosymposia, 2(1), 25–53. https://doi.org/10.11646/zoosymposia.2.1.6
- Boyle, M. J., & Seaver, E. C. (2008). Developmental expression of foxA and gata genes during gut formation in the polychaete annelid, Capitella sp. I. Evolution & Development, 10(1), 89–105. https://doi.org/10.1111/J.1525-142X.2007.00216.X
- Brenneis, G., Frankowski, K., MaaB, L., & Scholtz, G. (2023). The sea spider *Pycnogonum littorale* overturns the paradigm of the absence of axial regeneration in molting animals. *PNAS*, 120(5), e2217272120. https://doi.org/10.1073/pnas.221727120
- Brockes, J. P. (1997). Amphibian limb regeneration: Rebuilding a complex structure. *Science*, *276*(5309), 81–87. https://doi.org/10.1126/SCIENCE.276.5309.81

- Burns, R. T., Pechenik, J. A., Biggers, W. J., Scavo, G., & Lehman, C. (2014). The B vitamins nicotinamide (B3) and riboflavin (B2) stimulate metamorphosis in larvae of the deposit-feeding polychaete *Capitella teleta*: Implications for a sensory ligand-gated ion channel. *PLoS ONE*, 9(11), e109535. https://doi.org/10.1371/journal.pone.0109535
- Byrnes, E. F. (1904). Regeneration of the anterior limbs in the tadpoles of frogs. Archiv Für Entwicklungsmechanik Der Organismen, 18(2), 171–177. https://doi.org/10.1007/BF02163652
- Carnevali, C. (2006). Regeneration in echinoderms: Repair, regrowth, cloning. *Invertebrate Survival Journal*, 3(1), 64–76.
- Carnevali, M. D. C., Lucca, E., & Bonasoro, F. (1993). Mechanisms of arm regeneration in the feather star Antedon mediterranea: Healing of wound and early stages of development. Journal of Experimental Zoology, 267(3), 299–317. https://doi.org/10.1002/JEZ.1402670308
- Cary, G. A., Wolff, A., Zueva, O., Pattinato, J., & Hinman, V. F. (2019). Analysis of sea star larval regeneration reveals conserved processes of whole-body regeneration across the metazoa. *BMC Biology*, 17(1), 16. https://doi.org/10.1186/s12915-019-0633-9
- Chartier, T. F., Deschamps, J., Dürichen, W., Jékely, G., & Arendt, D. (2018). Whole-head recording of chemosensory activity in the marine annelid *Platynereis dumerilii*. Open Biology, 8(10), 180139. https://doi.org/10.1098/RSOB.180139
- Cohen, R. A., & Pechenik, J. A. (1999). Relationship between sediment organic content, metamorphosis, and postlarval performance in the deposit-feeding polychaete *Capitella* sp. I. *Journal of Experimental Marine Biology and Ecology*, 240, 1–18. https://doi.org/10.1016/ S0022-0981(99)00047-7
- Conzelmann, M., Williams, E. A., Tunaru, S., Randel, N., Shahidi, R., Asadulina, A., Berger, J., Offermanns, S., & Jékely, G. (2013). Conserved MIP receptor-ligand pair regulates *Platynereis* larval settlement. *Proceedings of the National Academy of Sciences of the United States of America*, 110(20), 8224–8229. https://doi.org/10.1073/PNAS.1220285110/-/DCSUPPLEMENTAL
- Cuvier, G., & Latreille, P. A. (1829). Le règne animal distribué d'après son organisation, pour servir de base à l'histoire naturelle des animaux et d'introduction à l'anatomie comparée. Chez Déterville. https://doi.org/ 10.5962/bhl.title.49223
- Dannenberg, L. C., & Seaver, E. C. (2018). Regeneration of the germline in the annelid *Capitella teleta*. *Developmental Biology*, 440(2), 74–87. https://doi.org/10.1016/j.ydbio.2018.05.004
- de Jong, D. M., & Seaver, E. C. (2016). A stable thoracic hox code and epimorphosis characterize posterior regeneration in *Capitella teleta*. *PLoS ONE*, 11(2), e0149724. https://doi.org/10.1371/journal.pone. 0149724
- de Jong, D. M., & Seaver, E. C. (2017). Investigation into the cellular origins of posterior regeneration in the annelid *Capitella teleta*. *Regeneration* (Oxford, England), 5(1), 61–77. https://doi.org/10.1002/reg2.94
- del Olmo, I., Verdes, A., & Alvarez-Campos, P. (2022). Distinct patterns of gene expression during regeneration and asexual reproduction in the annelid *Pristina leidyi*. *Journal of Experimental Zoology*, 338, 405–420. https://doi.org/10.1002/jez.b.23143
- Dill, K. K., & Seaver, E. C. (2008). Vasa and nanos are coexpressed in somatic and germ line tissue from early embryonic cleavage stages through adulthood in the polychaete Capitella sp. I. Development Genes and Evolution, 218(9), 453–463. https://doi.org/10.1007/s00427-008-0236-x
- Giani, V. C., Yamaguchi, E., Boyle, M. J., & Seaver, E. C. (2011). Somatic and germline expression of *piwi* during development and regeneration in the marine polychaete annelid *Capitella teleta*. *EvoDevo*, *2*(1), 10. https://doi.org/10.1186/2041-9139-2-10
- Grassle, J., & Grassle, J. F. (1976). Sibling species in the marine pollution indicator *Capitella* (polychaeta). *Science*, 192(4239), 567–569. https://doi.org/10.1126/science.1257794
- Hadfield, M. G. (2010). Biofilms and marine invertebrate larvae: What bacteria produce that larvae use to choose settlement sites. *Annual Review*

- of Marine Science, 3, 453-470. https://doi.org/10.1146/ANNUREV-MARINE-120709-142753
- Hadfield, M. G., Meleshkevitch, E. A., & Boudko, D. Y. (2000). The apical sensory organ of a gastropod veliger is a receptor for settlement cues. *Biological Bulletin*, 198(1), 67–76. https://doi.org/10.2307/ 1542804
- Harrison, R. G. (1898). The growth and regeneration of the tail of the frog larva studied with the aid of Born's method of grafting. *Archiv Für Entwickelungsmechanik Der Organismen*, 7(2–3), 430–485. https://doi.org/10.1007/BF02161494
- Hiebert, T. C., & Maslakova, S. (2015). Integrative taxonomy of the Micrura alaskensis Coe, 1901 species complex (Nemertea: Heteronemertea), with descriptions of a new genus maculaura gen. nov. and four new species from the NE pacific. Zoological Science, 32(6), 615-637. https://doi.org/10.2108/ZS150011
- Humphreys, T., Weiser, K., Arimoto, A., Sasaki, A., Uenishi, G., Fujimoto, B., Kawashima, T., Taparra, K., Molnar, J., Satoh, N., Marikawa, Y., & Tagawa, K. (2022). Ancestral stem cell reprogramming genes active in hemichordate regeneration. Frontiers in Ecology and Evolution, 10, 769433. https://doi.org/10.3389/fevo.2022.769433
- Jeffery, W. R. (2015). Regeneration, stem cells, and aging in the tunicate Ciona: Insights from the oral siphon. International Review of Cell and Molecular Biology, 319, 255–282. https://doi.org/10.1016/bs.ircmb. 2015.06.005
- Juliano, C. E., Swartz, S. Z., & Wessel, G. M. (2010). A conserved germline multipotency program. *Development*, 137(24), 4113–4126. https://doi. org/10.1242/DEV.047969
- Kostyunchenko, R. P. (2022). *Nanos* is expressed in somatic and germline tissue during larval and post-larval development of the annelid *Alitta virens*. *Genes*, 13, 270. https://doi.org/10.3390/genes13020270
- Kozin, V. V., & Kostyuchenko, R. P. (2015). Vasa, PL10, and Piwi gene expression during caudal regeneration of the polychaete annelid Alitta virens. Development Genes and Evolution, 225(3), 129–138. https://doi.org/10.1007/s00427-015-0496-1
- Lowry, R. (2023). vassarstats [online software]. http://vassarstats.net/ anova1u.html
- Luttrell, S. M., Su, Y. H., & Swalla, B. J. (2018). Getting a head with Ptychodera flava larval regeneration. Biological Bulletin, 234(3), 152–164. https://doi.org/10.1086/698510
- Meyer, N. P., Boyle, M. J., Martindale, M. Q., & Seaver, E. C. (2010). A comprehensive fate map by intracellular injection of identified blastomeres in the marine polychaete *Capitella teleta*. EvoDevo, 1(1), 8. https://doi.org/10.1186/2041-9139-1-8
- Meyer, N. P., Carrillo-Baltodano, A., Moore, R. E., & Seaver, E. C. (2015). Nervous system development in lecithotrophic larval and juvenile stages of the annelid *Capitella teleta*. Frontiers in Zoology, 12(1), 1–27. https://doi.org/10.1186/s12983-015-0108-y
- Meyer, N. P., & Seaver, E. C. (2009). Neurogenesis in an annelid: Characterization of brain neural precursors in the polychaete *Capitella* sp. I. Developmental Biology, 335(1), 237–252. https://doi.org/10.1016/J. YDBIO.2009.06.017
- Moss, N. (2018). Regeneration in the pilidium. [Master's thesis, University of Oregon]. University of Oregon Scholar's Bank. https://scholarsbank.uoregon.edu/xmlui/handle/1794/23138?show=full
- Nakano, H., Hibino, T., Oji, T., Hara, Y., & Amemiya, S. (2003). Larval stages of a living sea lily (stalked crinoid echinoderm). *Nature*, 421, 158–160. https://doi.org/10.1038/nature01236
- Nedved, B. T., Freckelton, M. L., & Hadfield, M. G. (2021). Laser ablation of the apical sensory organ of *Hydroides elegans* (Polychaeta) does not inhibit detection of metamorphic cues. *The Journal of Experimental Biol*ogy, 224(20), jeb242300. https://doi.org/10.1242/JEB.242300
- Oulhen, N., Heyland, A., Carrier, T. J., Zazueta-Novoa, V., Fresques, T., Laird, J., Onorato, T. M., Janies, D., & Wessel, G. (2016). Regeneration in bipinnaria larvae of the bat star *Patiria miniata* induces rapid and

- broad new gene expression. *Mechanisms of Development*, 142, 10-21. https://doi.org/10.1016/j.mod.2016.08.003
- Özpolat, B. D., & Bely, A. E. (2016). Developmental and molecular biology of annelid regeneration: A comparative review of recent studies. Current Opinion in Genetics & Development, 40, 144–153. https://doi.org/ 10.1016/j.gde.2016.07.010
- Özpolat, B. D., Sloane, E. S., Zattara, E. E., & Bely, A. E. (2016). Plasticity and regeneration of gonads in the annelid *Pristina leidyi. EvoDevo*, 7(22), 22. https://doi.org/10.1186/s13227-016-0059-1
- Pernet, B., Amiel, A., & Seaver, E. C. (2012). Effects of maternal investment on larvae and juveniles of the annelid *Capitella teleta* determined by experimental reduction of embryo energy content. *Invertebrate Biology*, 131(2), 82–95. https://doi.org/10.1111/j.1744-7410.2012. 00263.x
- Peterson, K. J., Cameron, R. A., & Davidson, E. H. (1997). Set-aside cells in maximal indirect development: evolutionary and developmental significance. *BioEssays*, 19(7), 623-631. https://doi.org/10.1002/bies. 950190713
- Pfeifer, K., Dorresteijn, A. W., & Fröbius, A. C. (2012). Activation of Hox genes during caudal regeneration of the polychaete annelid *Platynereis dumerilii*. Development Genes and Evolution, 222(3), 165–179. https://doi.org/10.1007/s00427-012-0402-z
- Phipps, L. S., Marshall, L., Dorey, K., & Amaya, E. (2020). Model systems for regeneration: *Xenopus. Development (Cambridge)*, 147(6), dev180844. https://doi.org/10.1242/DEV.180844/223048
- Planques, A., Malem, J., Parapar, J., Vervoot, M., & Gazave, E. (2019). Morphological, cellular and molecular characterization of posterior regeneration in the marine annelid *Playnereis dummerilli*. *Developmental Biology*, 445(189–210), 189–210. https://doi.org/10.10106/j.ydbio. 2018.11.004
- Porrello, E. R., Mahmoud, A. I., Simpson, E., Hill, J. A., Richardson, J. A., Olson, E. N., & Sadek, H. A. (2011). Transient regenerative potential of the neonatal mouse heart. *Science*, 331(6020), 1078–1080. https://doi.org/10.1126/science.1200708
- Rawls, A., & Olson, E. N. (1997). *MyoD* meets its maker. *Cell*, *89*(1), 5–8. https://doi.org/10.1016/S0092-8674(00)80175-0
- Reddien, P. W. (2018). The cellular and molecular basis for planarian regeneration. Cell, 175(2), 327–345. https://doi.org/10.1016/j.cell. 2018.09.021
- Reddy, P. C., Gungi, A., & Unni, M. (2019). Cellular and molecular mechanisms of hydra regeneration. *Results and Problems in Cell Differentiation*, 68, 259–290. https://doi.org/10.1007/978-3-030-23459-1_12
- Schindelin, J., Arganda-Carreras, I., Frise, E., Kaynig, V., Longair, M., Pietzsch, T., Preibisch, S., Rueden, C., Saalfeld, S., Schmid, B., Tinevez, J. Y., White, D. J., Hartenstein, V., Eliceiri, K., Tomancak, P., & Cardona, A. (2012). Fiji: An open-source platform for biological-image analysis. *Nature Methods* 2012 9:7, 9(7), 676–682. https://doi.org/10.1038/nmeth.2019
- Schoeman, S., & Simon, C. A. (2023). Live to die another day: Regeneration in *Diopatra aciculata* Knox and Cameron, 1971 (Annelida: Onuphidae) collected as bait in Knysna estuary, South Africa. *Biology*, 12(3), 483. https://doi.org/10.3390/biology12030483
- Seaver, E. C. (2022). Sifting through the mud: A tale of building the annelid Capitella teleta for EvoDevo studies. Current Topics in Developmental Biology, 147, 401–432. https://doi.org/10.1016/BS.CTDB.2021. 12.018
- Seaver, E. C., Thamm, K., & Hill, S. D. (2005). Growth patterns during segmentation in the two polychaete annelids, *Capitella* sp. I and *Hydroides elegans*: Comparisons at distinct life history stages. *Evolution Development*, 7(4), 312–326. https://doi.org/10.1111/j.1525-142X.2005.05037.x
- Singer, M. (1954). Induction of regeneration of the forelimb of the postmetamorphic frog by augmentation of the nerve supply. *Journal of Experimental Zoology*, 126(3), 419–471. https://doi.org/10.1002/jez. 1401260304

- Social Science Statistics T-Test Calculator for 2 Independent Means. (2023). Retrieved from https://www.socscistatistics.com/tests/studentttest/default2.aspx
- Stewart, B. (1998). Sub-lethal predation and rate of regeneration in the euryalinid snake star Astrobrachion constrictum (Echinodermata, Ophiuroidea) in a New Zealand fiord. Journal of Experimental Marine Biology and Ecology, 199(2), 269–283. https://doi.org/10.1016/0022-0981(95)00177-8
- Sur, A., Magie, C. R., Seaver, E. C., & Meyer, N. P. (2017). Spatiotemporal regulation of nervous system development in the annelid *Capitella* teleta. EvoDevo, 8, 13. https://doi.org/10.1186/s13227-017-0076-8
- Takeo, M., Yoshida-Noro, C., & Tochinai, S. (2008). Morphallactic regeneration as revealed by region-specific gene expression in the digestive tract of *Enchytraeus japonensis* (Oligochaeta, Annelida). *Developmental Dynamics*, 237(5), 1284–1294. https://doi.org/10.1002/dvdy.21518
- Vickery, M. C. L., Vickery, M. S., Amsler, C. D., & McClintock, J. B. (2001). Regeneration in echinoderm larvae. *Microscopy Research and Technique*, 55(6), 464–473. https://doi.org/10.1002/jemt.1191
- Vickery, M. S., & McClinktock, J. B. (1998). Regeneration in metazoan larvae. *Nature*, 394, 140. https://doi.org/10.1038/28086
- Vickery, M. S., Vickery, M. C. L., & McClintock, J. B. (2002). Morphogenesis and organogenesis in the regenerating planktotrophic larvae of asteroids and echinoids. *Biological Bulletin*, 203(2), 121–133. https://doi. org/10.2307/1543381
- Walters, B. J., & Zuo, J. (2013). Postnatal development, maturation and aging in the mouse cochlea and their effects on hair cell regeneration. *Hearing Research*, 297, 68–83. https://doi.org/10.1016/j.heares.2012. 11.009
- Yamaguchi, E., Dannenberg, L. C., Amiel, A. R., & Seaver, E. C. (2016). Regulative capacity for eye formation by first quartet micromeres of the polychaete *Capitella teleta*. *Developmental Biology*, 410(1), 119–130. https://doi.org/10.1016/j.ydbio.2015.12.009
- Yamaguchi, E., & Seaver, E. C. (2013). The importance of larval eyes in the polychaete *Capitella teleta*: Effects of larval eye deletion on formation of the adult eye. *Invertebrate Biology*, 132(4), 352–367. https://doi.org/10.1111/jvb.12034
- Yun, M. (2015). Changes in regenerative capacity through lifespan. *International Journal of Molecular Sciences*, 16(10), 25392–25432. https://doi.org/10.3390/ijms161025392

- Zammit, P. S. (2017). Function of the myogenic regulatory factors *Myf5*, *MyoD*, *Myogenin* and *MRF4* in skeletal muscle, satellite cells and regenerative myogenesis. *Seminars in Cell & Developmental Biology*, 72, 19–32. https://doi.org/10.1016/J.SEMCDB.2017.11.011
- Zattara, E. E., & Bely, A. E. (2013). Investment choices in post-embryonic development: Quantifying interactions among growth, regeneration, and asexual reproduction in the annelid *Pristina leidyi*. *Journal of Experimental Zoology Part B: Molecular and Developmental Evolution*, 320(8), 471–488. https://doi.org/10.1002/jez.b.22523
- Zattara, E. E., & Bely, A. E. (2016). Phylogenetic distribution of regeneration and asexual reproduction in *Annelida*: Regeneration is ancestral and fission evolves in regenerative clades. *Invertebrate Biology*, 135(4), 400–414. https://doi.org/10.1111/IVB.12151
- Zattara, E. E., & Fernández-Alvarez, F. A. (2022). Collecting and culturing Lineus sanguineus to study Nemertea WBR. In S. Blanchoud & B. Galliot (Eds.), Whole-body regeneration: Methods and protocols. Humana. 10.1007/978-1-0716-2172-1
- Zattara, E. E., Fernández-Álvarez, F. A., Hiebert, T. C., Bely, A. E., & Norenburg, J. L. (2019). A phylum-wide survey reveals multiple independent gains of head regeneration in Nemertea. *Proceedings of the Royal Society B: Biological Sciences*, 286, 20182524. https://doi.org/10.1098/rspb.2018.2524
- Zou, J., Wu, X., Shi, C., Zhong, Y., Yan, Q., Su, L., & Li, G. (2021). A potential method for rapid screening of amphioxus founder harboring germline mutation and transgene. Frontiers in Cell and Developmental Biology, 9, 702290. https://doi.org/10.3389/fcell.2021.702290

How to cite this article: Boyd, A. A., & Seaver, E. C. (2023). Investigating the developmental onset of regenerative potential in the annelid *Capitella teleta*. *Invertebrate Biology*, e12411. https://doi.org/10.1111/ivb.12411